QUANTIFYING THE EFFECTS OF CURING STRESSES AND SOIL TYPE ON THE IN-SITU COMPRESSIVE STRENGTH OF CEMENT-TREATED SOILS VIA DEEP MIXING METHOD

by

George A. Onorato

A thesis submitted to the Faculty and the Board of Trustees of the Colorado School of Mines in partial fulfillment of the requirements for the degree of Master of Science (Civil and Environmental Engineering).

Golden, Colorado

Date ____________________

Signed: ______________________

George A. Onorato

Signed: ______________________

Dr. Ning Lu

Thesis Advisor

Golden, Colorado

Date: ______________________

Signed: ______________________

Dr. Junko Munakata Marr

Department Head and Professor,

Civil and Environmental Engineering

ABSTRACT

The Deep Mixing Method (DMM) is an ever-growing ground improvement technique used worldwide to improve in-situ soils using cementitious binders and/or other types of admixtures to either increase the strength and/or decrease the permeability of soils for various types of civil and/or environmental engineering applications. The process involves using specialized high torques drilling equipment with specially design augers or cutters that allow for the injection of flowable grout (suspension) through the auger or cutter to liquify the soil in-situ while blending in the cementitious suspension. When the suspension and soil mixture solidify, the designed engineering material properties are achieved. This study investigates the curing conditions in which in-situ materials are exposed to and how these conditions influence the strength of the deep mixed materials. The findings of this study reveal that the curing conditions for in-situ materials, particularly the applied stresses and temperatures, differ significantly from the conditions under which typical quality control specimens are cured. Consequently, these conditions can lead to a significant underestimation of the strength of the in-situ materials if curing conditions are not considered.

This study incorporates field and laboratory data collected from various studies that directly or indirectly studied the influences of curing stresses on deep mixed material's mechanical properties. The data compiled for this investigation included strength and temperature data derived from specially designed laboratory bench test studies, field conducted modified oedometer tests, in-situ instrumentation tests from deep mixed columns, and a review of independent coring data results from datasets collected from deep mixed project across north America. Upon reviewing these collective studies, it becomes evident that there exists a correlation between curing stress and unconfined compressive strength (UCS). The observed rate of strength gains follows a linear pattern and is influenced by the type of soil being treated. Notably, fine-grain soils exhibit a higher rate of strength gain when subjected to in-situ curing stress (with depth) in comparison to granular soils. Additionally, this study puts forth several hypothesized physio-chemical mechanisms that could potentially explain the varying strength gains observed based the influence of the treated soil's particle size.

TABLE OF CONTENTS

LIST OF FIGURES

LIST OF TABLES

ACKNOWLEDGEMENTS

I would like to acknowledge the support and my sincere gratitude to my advisor Dr. Ning Lu and committee members Dr. Alexandra Wayllace and Dr. Michael Mooney for their academic guidance throughout my graduate studies at Mines.

I would also like to express my deepest gratitude to Dr. Giovanni Bonita, P.E., P.G. and Dr. Jesus Gomez, P.E. for their guidance, support, and encouragement while I pursued my curiosity with this research.

I would also like to acknowledge the financial support provided by the Deep Foundations Institute (DFI) and GEI Consultants, Inc. A significant portion of the referenced data within this thesis was derived through the DFI's Technical Committee Project Fund where I served as the principal investigator (PI) along with my advisor and co-author Dr. Giovanni Bonita, P.E., P.G.

I would also like to express appreciation for the collaboration from the following individuals: Mark Ahrens, Dr. Michael Arnold., Dr. George Filz, P.E., Asher Peltz, P.E., and Brain Wilson, P.Eng. This work could not have been possible without all your support.

CHAPTER 1
INTRODUCTION

The deep mixing method (DMM) is a soil treatment technique that involves blending soil with cementitious grout to create "soil cement" with enhanced mechanical properties. It finds various applications in modern civil engineering, including ground improvement, excavation support, groundwater containment, dam reinforcement, and environmental protection. However, accurately measuring the performance of these materials in their in-situ conditions poses challenges.

Current quality control (QC) testing methods for soil-cement materials produced by deep mixing rely on wet grab samples or direct coring. However, both methods have limitations. Coring can lead to micro-fracturing or damage to specimens, particularly if the treated soil contains gravel, cobbles, or shell fragments. Wet grab samples, although easier to obtain, may be inadvertently screened during retrieval, potentially altering the specimen's composition (FHWA, 2013). Additionally, wet grab specimens are prepared and cured at surface conditions, which differ from in-situ conditions involving overburden stress and elevated temperatures. In practice, the influence of in-situ curing conditions on the material strength is typically overlooked, which leads to an underestimation of actual in-situ strengths of the treated soils. This oversight can have significant monetary consequences on a project. It can lead to expensive rework of ground improvement, based on compromised or lower than expected QC results. Additionally, it can result in unnecessary expenditures associated with excessive use of binder/admixture materials on a project.

To initiate the study aimed at comprehending and quantifying the impact of total overburden stresses on strength development throughout the curing process, it is essential for the investigation to first grasp the nature of internal stresses during curing and their potential influence on drainage, consolidation, soil structure reorientation, and cement chemical bonding process. Additionally, by quantifying the impact of curing conditions on the strength of soil-cement materials, engineers are provided with an additional tool to enhance their ability to assess quality control data within a project.

1.1 Research Objectives and Questions

The primary aim of this project was to investigate with the purpose of gaining a deeper understanding of the total internal stress present within a freshly mixed column, and to explore how these stresses, specifically the total overburden stress, influence the in-situ strength of a cement-treated soils. A brief background explaining the nuances associated with these objectives is presented in this chapter. Following the background, are questions that were developed to address the objectives of this research.

The study of deep mixed materials poses numerous challenges because of the diverse array of factors that can influence material properties. These factors encompass a wide range, from the heterogeneous characteristics of ground conditions to deliberate or unintentional variations in binder proportions. The extent of these variations can be considerable, spanning across an entire site or even within a single deep mixed component. Understanding the challenges surrounding the study of deep mixed materials is crucial due to the significant impact that confounding variables can have on material properties. Confounding variables play a critical role in this research as they can introduce bias and impact the validity of experimental results and influence the relationship between the independent and dependent variables. Recognizing these challenges is essential to try and capture the fundamental nature and behavior of these materials.

The following questions were developed to address the objectives of this research:

1. *What are the internal total and effective stresses within a deep mixed column and how do they change throughout the curing process?* Given the loose unconsolidated state of the material once freshly mixed with grout, it is hypothesized that internal drainage and consolidation occurs until the cement hydration process stiffens the bonds between soil particles to a point that this process finally ceases. For a more comprehensive comprehension of this process, an assessment of in-situ stresses is undertaken through instrumentation measurements taken from freshly mixed columns. Additionally, a study conducted by Hayashi et al. (2005), which delves into the consolidation characteristics of cement-treated soil in its initial state, is reviewed.

2. *What influence does curing stress have on the strength of deep mixed materials?* Based on a literature search, limited research has been conducted on studying the influence of

curing stresses on the properties of deep mixed materials. The primary reason for this scarcity is the requirement for specialized testing equipment that can simulate in-situ conditions while allowing the specimen to maintain its shape during the curing process. A triaxial loading apparatus would be capable of applying an appropriate load; however, the flexible membrane used in this apparatus tends to deform the specimen as confinement stresses are applied. Alternatively, a standard oedometer cell is rigid enough but generally not designed to contain a wet consistency material and too small in dimensions to make a direct comparison against typical formed concrete test cylinders. Onorato and Bonita (2020) addressed this issue by developing a modified oedometer cell specifically tailored to handle wet soil-cement materials. This apparatus enabled the molding of specimens that match the dimensions of a standard 3-inch by 6-inch test cylinder. Furthermore, the modified oedometer cell allows for specimen consolidation and drainage under an applied axial dead load. This apparatus was key for developing experiments to study the influence that curing stresses on cement-treated soils strength. Onorato and Bonita (2023) summarized the results of several controlled bench tests and field tests using the modified oedometer that have been evaluated for this project to help draw a conclusion to this question.

3. *Under curing stress, does grain size and plasticity of the treated soil affect the strength of the deep mixed material?* To investigate the influence of grain size and plasticity on the strength of cement-treated soil under curing stresses, data from various sources were reviewed and organized based on soil type using USCS classifications. Subsequently, the sorted data was evaluated to identify unique strength trends.

4. *What are the hydration temperatures within a deep mixed columns and do they differ from specimens cured within a typical QC test cylinder?* Curing temperature is recognized as a significant factor that impacts the strength of cement-treated soil. Numerous researchers have reported an increase in unconfined compressive strength (UCS) with higher curing temperatures (Bruce et al., 2013; Hirabayashi et al., 2009; Zhang et al., 2014). To investigate the differences in curing temperature, a review of temperature measurements collected from in-situ deep mixed columns is compared

against heat of hydration temperature readings from a controlled laboratory bench test where cement-treated soil specimens were cured under typical laboratory settings.

1.2 Thesis Overview and Organization

This study aims to investigate and understand the behavior and properties of deep mixed materials, specifically focusing on the influence of curing stresses. The research adopts a systematic approach by comprehensively reviewing diverse sets of data from various sources. These sources encompass controlled laboratory bench studies, field-cured experiments using a modified oedometer, field in-situ instrumentation tests, and data obtained from deep mixed projects through random coring tests.

To ensure the accuracy and reliability of the findings, the approach involves carefully examining all the data sources. This includes identifying and eliminating confounding variables that are inherent to deep mixed materials. By addressing these variables, the study aims to isolate and highlight the genuine correlations and trends that are consistent across different data sources. Through this analysis, the research strives to identify common patterns and associations among the data sources. This approach allows for the identification of meaningful relationships and trends that transcend individual studies or experiments. By considering a broad range of data and systematically removing confounding variables, the research aims to provide a comprehensive understanding of the strength gaining behavior of deep mixed materials that are cured in-situ under overburden stresses.

Firstly, in Chapter 2 a comprehensive literature search is conducted to gather existing knowledge and identify any gaps in the understanding of deep mixed materials under curing stresses. This provides a foundation for the study and helps establish the research context.

Chapter 3 provides a summary of the data reviewed for this research that includes data derived from the modified oedometer cell to simulate in-situ conditions during the curing process. This apparatus enables the examination of the material's response and properties under controlled curing stresses. The modified oedometer was used to generate critical data for laboratory bench tests as well as field tests from active sites across the country. In addition, this Chapter also summarizes results from in-situ instrumentation tests as well as the downsized coring data. Chapter 4 summarizes the data validation criteria and the statistical tools used to assess the quality of the data included in this study.

Chapter 5 discusses the results of the study and is divided into five subsection that include a discussion on the influence of curing stress on UCS values, a comparison of in-situ versus laboratory test cylinder temperature evolution, a review of an analysis of the effects of the water to cement ratio on UCS in consolidated samples, and influence of consolidation on strength.

Chapter 6 presents conclusions obtained from a review of the data and analysis, and finally, Chapter 7 discusses recommendations for future research.

Appendices A.1 includes Coauthor's Permission and A.2 includes permissions to use figures, tables, and data from other publications.

CHAPTER 2

LITERATURE REVIEW

This chapter provides a comprehensive literature review of key components relevant to the present research. The review focuses on several important topics that have a direct bearing on the study's objectives. These main topics include the effects of confinement stress during curing and consolidation behavior of cement-treated soils in their fresh state is also examined. This aspect explores how the material undergoes consolidation during the curing phase, which provides insight into the strength gaining behavior. Finally, this literature review includes some information on the topic of in-situ curing temperatures in deep mixed columns. While curing temperatures is not a primary objective of this thesis, it is a relevant curing condition and helps to provide essential context for evaluating instrumentation temperature data.

2.1 Effects of Curing Stress on UCS

In the past decades, substantial research has been devoted to understanding soil mixed material properties, as evidenced by studies conducted by Filz et al. (2005), Bruce et al. (2013), Kitazume et al. (2013), Suzuki et. al. (2014), Nevarez-Garibaldi et al. (2018), and many others; however, until recently there has been relatively limited research surrounding the understanding of the effect of curing stress (i.e., overburden stress) on cement-treated soil's mechanical properties. In the few studies that were conducted, the studies were relatively small in scope with respect to the range of overburden stresses evaluated and typically performed using only one soil type. These limitations overlook important trends that exist across different soil types and under variable field conditions. Onorato and Bonita (2020) pioneered an approach to study this the influence of curing stressed by conducted a comprehensive study that presented preliminary data on the influence of curing stresses over multiple soil types and included data from both field and laboratory conditions. This data showed a strong linear relationship between overburden stress and UCS values between all data sources evaluated from both the laboratory and field. The conclusions drawn in Onorato and Bonita's (2020) report implied a relationship between the rate of strength gain (Δq_u) and the treated soil types, in which they present data that suggested that cement-treated fine-grain soils showed greater strength gains than granular soils. A brief background on the conclusions of these studies is discussed below.

One of the earliest studies on the influence of curing stresses on the strength of cement-treated sands was conducted by Yamamoto et al. (2002). The paper was written in Japanese; however, the results of their study were published by Kitazume and Terashi (2013) in a book titled "*Deep Mixing Method*". Their results show that the strength increased almost linearly with overburden stress irrespective of the type and amount of binder used. Figure 2.1 shows the relationship of overburden stress to UCS values on cement-treated sandy soils. The figure also shows the strength of the stabilized sands having different initial water content.

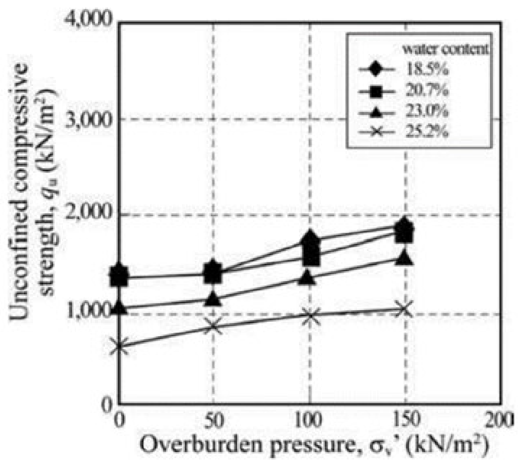

Figure 2.1 Relationship between unconfined compressive strength, q_u and overburden stress, σ'_v (*Yamamoto et al., 2002*)

In a related study, Rabbi et al. (2011) conducted experiments using a poorly graded sand (SP) as a base soil type and concluded that the addition of confining stress during curing had an increasing effect on the peak strength, stiffness Young's Modulus (E_v) and Shear Modulus (G_{vh}), and in the post peak properties of the material. Rabbi et al. also concluded that typical testing techniques used to evaluate cement-treated soil provided an underestimation of stress-stain behavior of cement-treated sand. These results were also concurred by Taher et al. (2011) in a related study.

As part of a master's thesis, Starcher (2013) conducted experiments evaluating the effect of vertical stress during curing for a soil-cement mixture that included a laboratory fabricated soil of kaolin (CL) and fine Nevada sand (SW) mixed at a 1:1 ratio, thus classifying the base soil type as a sandy lean clay (SC) using United Soil Classification System. The study involved a series of consolidation tests and unconfined compression tests, with special attention paid to the effects of curing time and vertical curing stress. Starcher (2013) concluded that unconfined compressive strength of the soil-cement mixture increased with curing time and with vertical confining stress. In addition, Starcher also reported that an increase in elastic moduli (E_v) of 100 to 1,000 percent was observed when compared to specimens tested without curing stresses.

Suzuki, et al. (2014) also published results of peak and residual strength characteristics of cement-treated soil cured under different consolidation conditions. While their study specifically focused on undrained shear strength under different loading conditions (isotropic and one-dimensional consolidation), they did present results for unconfined compressive strength versus applied curing stress which was reported in their paper. Based on the published grain size distribution data, it appears that Suzuki et al. used a mixture of granular and fine grain soil (SC-CL) from Yamaguchi City as a base soil type. The prepared soil-cement mixture utilized a standard Portland Cement at a 50 kg/m^3 binder rate with a water to cement ratio of 1.6. and cured their specimens using applied curing stresses ranging between 7- and 21-pound per square inch (psi). Their results showed a clear increase in both shear and compressive strength with applied curing stress for both isotropic and one-dimensional loading and concluded that tests conducted without consideration for in-situ stress would underestimate undrained shear strength in the field.

In the broadest study conducted until this point, Onorato and Bonita (2020) published preliminary results of their observations on the influence of curing stresses on cement-treated soil unconfined compressive strength for different treated soil types by collecting data across several sources including both laboratory and field study sources. The primary unit of measurement introduced by this study to evaluate the change in unconfined compressive strength (q_u) as a function of overburden curing stress (σ_z) was defined as the rate of strength change (Δq_u) and is described as Equation 2.1.

$$\Delta q_u = \frac{(q_{u,z} - q_{u,0})}{q_{u,0}} \tag{2.1}$$

Where, Δq_u is the rate of strength change and $q_{u,0}$ is the measured unconfined compressive strength cured with no overburden stress, and $q_{u,z}$ is the unconfined compressive strength at depth (z) confinement stress. It was also suggested in their study that the applied confinement stress (σ_z) during curing is equal to the total vertical overburden stress (σ_v) at depth (z) within a deep mixed column: therefore, Onorato and Bonita (2020) defined curing stress as the unit weight of the wet mixed material times the overburden depth, as shown in Equation 2.2.

$$\sigma_z(\mathrm{z}) = \gamma_{sat,mix}(z) \tag{2.2}$$

Where, σ_z is equal to vertical overburden pressure (curing stress), σ_v at depth z, $\gamma_{sat,mix}$ is the saturated unit weight of the wet mixed soil-cement material, and z is the depth. To show the relationship between overburden stress, σ_z and the rate of change in unconfined compressive strength (Δq_u), a controlled laboratory bench test (BT-1) was conducted by preparing a soil-cement mixture that used well graded sand (SW) as the base treated soil. Four specimens were formed from the same soil-cement mixture, and each were cured under different confinement stresses using a specially designed modified oedometer cell. The results correlated well with the findings presented by Yamamoto et al. (2002) showing a near perfect linear relationship in both unconfined compressive strengths to overburden curing pressure (Figure 2.2a) and the rate of strength change (gain) to the overburden curing pressure (Figure 2.2b).

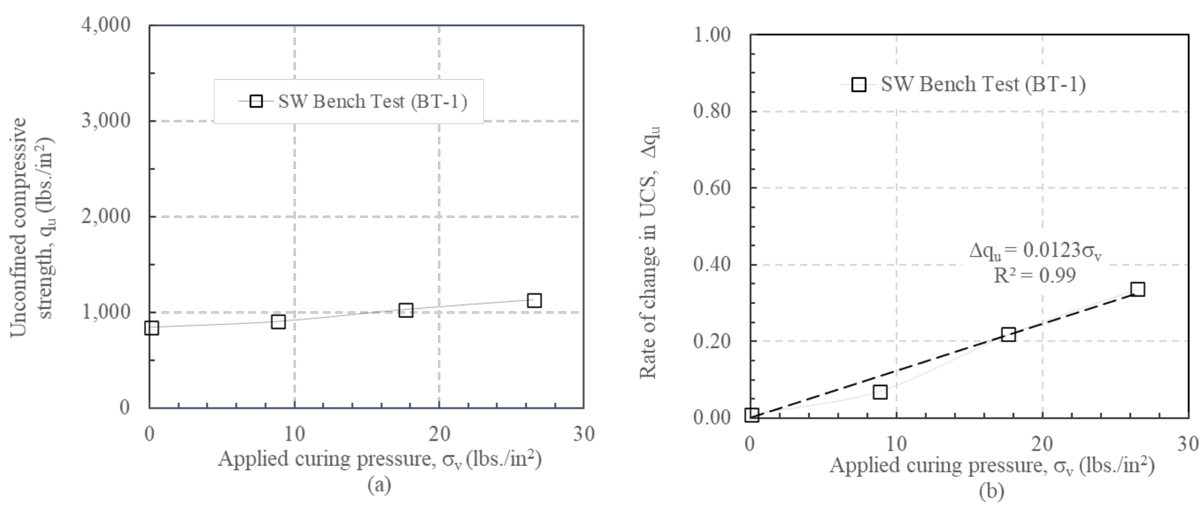

Figure 2.2 Relationships between overburden pressure and UCS (a) and overburden pressure and rates of change in UCS (b).

Onorato and Bonita (2020) also showed in their initial study that soil types (grain sizes) had an influence on the rate of which strength is gained (Δq_u). This dependence on soil type was observed through the collection of a broad set of field-derived data that evaluated strength data over several different soil types. This data included both field-stressed results obtained through a modified oedometer apparatus at four different deep mixed sites across US and Canada, and core run strength data obtained from an additional four deep mixed sites. In both data sets, a relationship between σ_v and Δq_u's dependence on soil type was also observed. In the case of the oedometer field-stress data, simulated overburden pressures were applied consistent with Equation 2.2, and in the case of the core run data, recovered core materials were cured in-situ under natural overburden stresses.

Figure 2.3a shows the relationships of applied curing stresses (overburden stress) to the rate of strength gains shown with the best least-squared fit lines and R^2 value for the field-stressed data, sorted by soil types; and Figure 2.3b presents the same results for the coring sites evaluated.

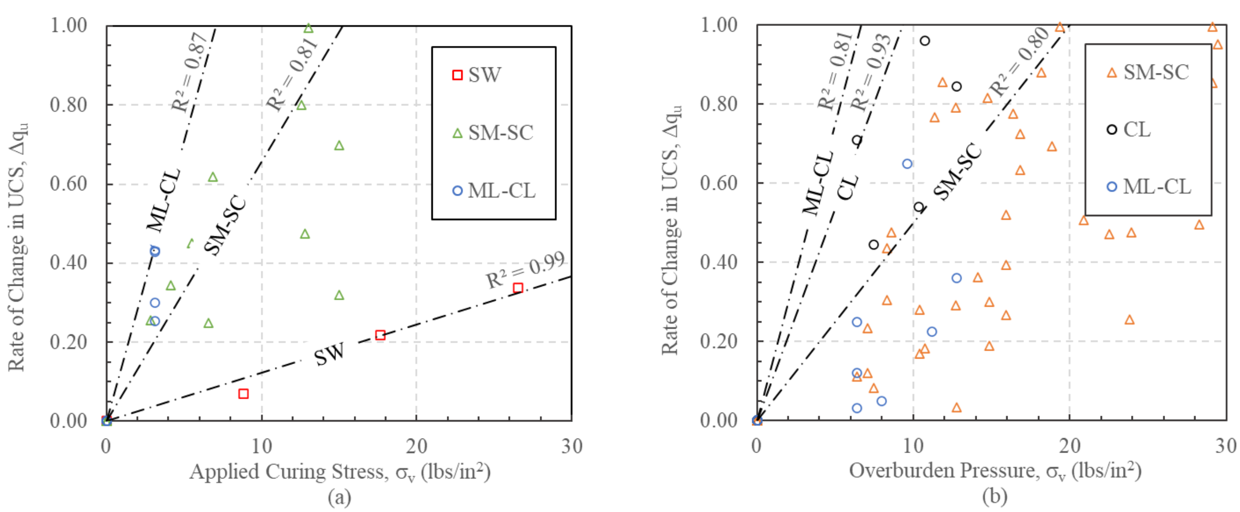

Figure 2.3 Relationship between curing stress and rate of strength gain for different soil types for (a) oedometer field-stresses data and (b) core run data.

Figures 2.3a and 2.3b demonstrate clear and significant correlations between soil types, as shown by the linear regressions of the strength gain data. In both datasets evaluated, finer grain soils exhibited a much greater rate of strength gains than granular soils.

2.2 Comparison of Research Data

Figure 2.4 shows the relationships between curing stresses and the rate of strength gains, Δq_u for different base soil types that were treated in each of the published research discussed in Section 2.1. In summary, Yamamoto et al. (2002) used mainly a granular well graded sand with some clay (SW-SC), Starcher (2013) used a 1:1 mixture of sand and clay (SC), Suzuki (2014) used mainly fine grain clayey sand with some lean clay (SC-CL), and Onorato and Bonita used a granular well graded sand (SW) for their study. Equation 2.1 was used to normalize the unconfined compressive strength results to compare the rate of strength gains in each of these studies.

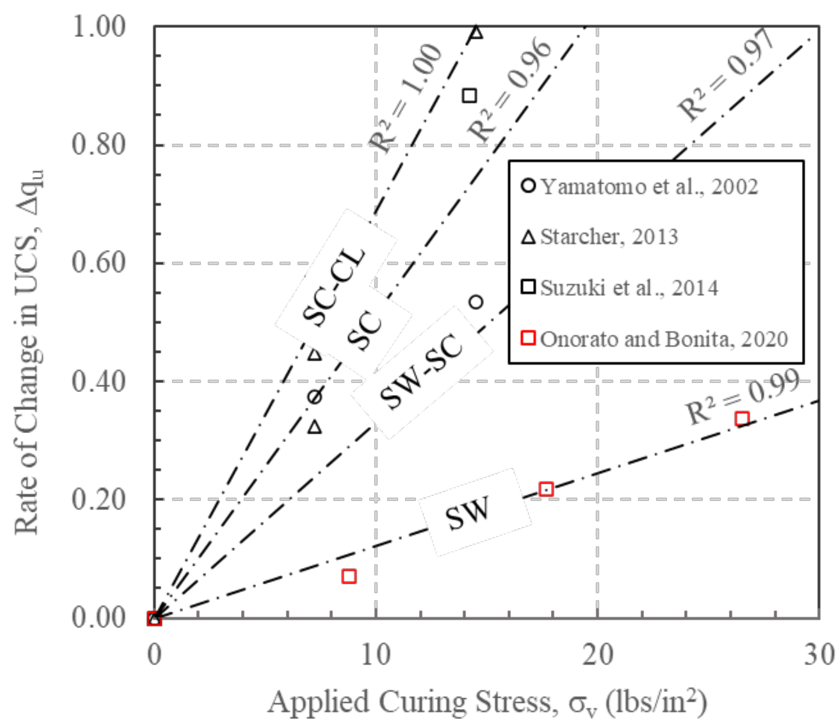

Figure 2.4 Relationship between curing stress and rate of strength gain for different soil types for published research.

A comparison of published research is consistent with the results presented by Onorato and Bonita (2020) showing a clear relationship that the treatment using finer grain soils exhibit greater rates of strength gains than cement-treated granular soils. The rate of strength gains appears to be subtly increasing depending on the amount of fines present in the mixture, implying a direct relationship with grain-size surface area and distribution.

2.3 Consolidation Behavior of Cement-treated Soils

Hayashi et al. (2002) conducted a study that centered around the consolidation behavior of cement-treated soils in their fresh state. It is hypothesized that the consolidation and drainage process during the initial stages of treatment enables the mechanisms responsible for the observed strength gains. Figure 2.5 shows how Hayashi et al. (2002) conceptualization the changes in effective overburden stress (σ'_v) and void ratio (e) changes with curing term.

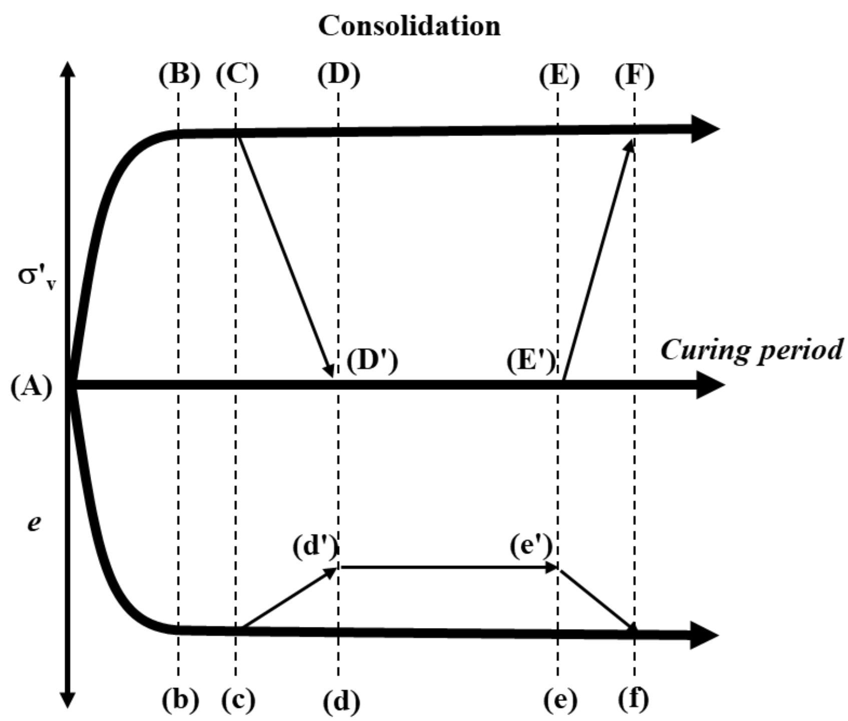

Figure 2.5 Effective overburden stress and void ratio changes during curing (*Hayashi et al., 2002*)

Hayashi et al. (2002) assumed that cement treatment initiates at point A and proposed that the consolidation yield stress (in-situ) follows a path from point A to point F, indicating a delay in the transfer of yield stress to the soil particles. The study suggested that this delay is influenced by the hydraulic conductivity properties of the treated soil types and the distance of the drainage path of the specimen. As a result, it was concluded that in the case of thick layers of high plasticity clays, consolidation in the fresh state may be disregarded when applying cement treatment, as the drainage process would be too slow to effectively consolidate the cement-treated materials in-situ before the cement reaction solidifies the material.

2.4 Effect of Curing Temperatures on UCS

There have been many studies on the influence of curing temperature on concrete strength, both in the general industry and for deep mixed soils treated with cement. Hirabayashi et al. (2009) and others have shown that high curing temperatures for deep mixed soils can accelerate the hydration reactions, thereby producing higher UCS values. However, an increase in strength seems to be apparent only at short-term curing times and less apparent at longer curing times (Kim et al., 1998). Filz et al. (2018) also suggested that curing temperatures of cement-treated soil are affected by the temperatures of the surrounding ground, which can retain heat in situ with temperatures over 100°C for up to two months after the deep mixed column is created.

While the scope of this study does not necessarily evaluate the effect of temperature on UCS values, this topic does represent a significant difference in curing conditions between deep mixed materials cured in-situ versus specimens cured in a laboratory and therefore should at discussed. This report presents temperature data that compares the differences in curing temperatures from deep mixed materials cured both in the ground and specimens cured within typical concrete test cylinders. As part of this study, a simple look at the differences in temperature readings will be evaluated from data obtained between these two curing conditions.

CHAPTER 3
DATA COLLECTION PROGRAM

Contents of this chapter are published in the Deep Foundations Institute (DFI) Technical Committee Project Reports, authored by Onorato and Bonita (2020/2023). The objective of the data collection program was to gather a diverse range of results, including laboratory studies and field-derived data, covering various soil types. This approach aimed to achieve a better understanding of the influences under different conditions. By incorporating a broad spectrum of data, we can obtain a comprehensive perspective on the impact of curing stress in real field conditions.

Data collection for this study comprised datasets from four main sources. Firstly, laboratory bench tests were conducted with measured and well understood physical properties, stresses, and composition of the cement-treated soil mixtures. Secondly, field-stressed data was obtained using modified oedometer cells, where the physical properties of the soils being treated and the composition of the soil-cement mixtures were approximate, but the stresses were known. To facilitate the study on these two data sources, a modified field oedometer cell was specially fabricated for this study as to allow for the application of specific overburden pressures onto freshly mixed cement-soil mixtures while the mixtures cured. Details of the design and utilization of this apparatus are described in Section 3.1.

In addition, field post-construction core run strength data was collected to serve as a comparative data source. Although the coring datasets provide only approximate information on soil properties and composition of the mixtures at recovery depths, they represent in-situ materials cured under overburden stresses. Therefore, analyzing trends in the strength data from the core samples proves valuable for comparison with the other datasets.

Lastly, in-situ instrumentation data was gathered from freshly mixed columns, recording in-situ stresses and temperatures during the curing process of soil-mixed columns. The collection of all four datasets is described in the following section.

3.1 Modified Field Oedometer

Onorato and Bonita (2020) introduced specialized modified oedometer cells that were specifically designed for studying the influence of curing stresses on cement-treated soils under varying overburden stress conditions. These cells could be utilized either in a laboratory or in the field, as they were designed to be easily set up at any field trailer on an active deep mixing project, making it convenient for on-site study using field-produced materials.

The equipment played a crucial role in subjecting a freshly mixed soil-cement specimen to an overburden stress, replicating the conditions experienced in the field. By applying a static axial load, the specimen could cure under these simulated in-situ conditions. This apparatus proved to be an essential tool for analyzing the effects of curing stresses on cement-treated soils and gaining valuable insights into their consolidation behavior while the specimens cured under a load.

The apparatus consists of a thin-walled clear confining chamber placed within a thick-walled outer restraining cradle, providing support to the confining chamber. A plunger head containing a coarse porous stone underneath is positioned within the chamber against the top of the specimen, allowing the porous stone to move in conjunction with the consolidation of the specimen. Another porous stone is placed beneath the wet specimen allowing drainage from both the top and bottom of the specimen. To load the test specimen, axial pressure is applied externally using a level arm and weights so that the total load to piston shaft can be adjusted at a specified overburden pressure.

The cell chamber is designed to allow free drainage of excess fluid pressure while the specimen consolidates and cures. The cell chamber is transparent, enabling direct monitoring of height changes as the specimen undergoes consolidation. The time-rate of consolidation can be monitored manually using vertical graduated scale, enabling measurement of changes in specimen height at 0.1-inch increments within the cell chamber. Differences in specimen height is logged manually while the consolidation occurs. Typically, specimens are monitored for at least five hours after a load is placed. After five hours, consolidation of the specimen is usually complete. Figure 3.1 shows a schematic diagram depicting the apparatus and its various components.

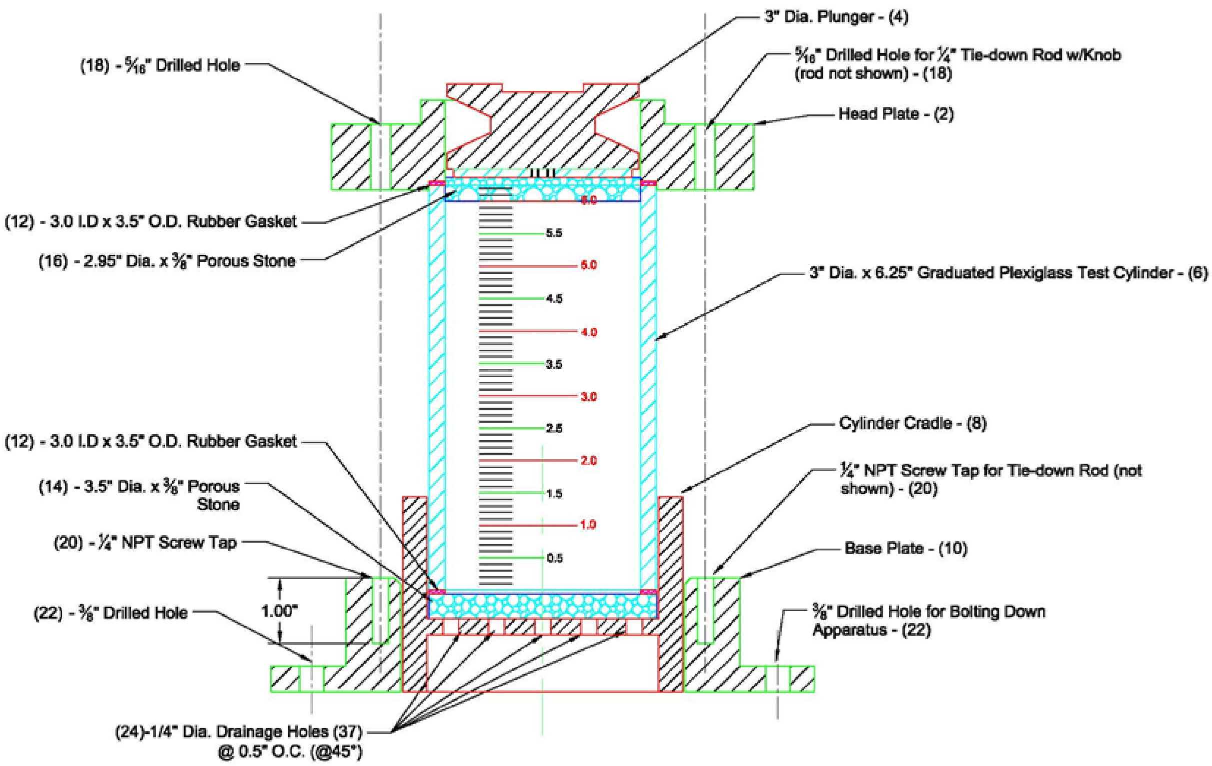

Figure 3.1 Cross-Section of modified oedometer cell (*Onorato and Bonita, 2020)*

3.2 Laboratory Bench Test Data

Bench tests on soil-cement materials have proven to be an important tool for evaluating the influence of curing conditions on the material strength. These laboratory tests allow for the accurate measurements and assessment of material behavior and engineering properties under relatively controlled conditions. The empirical relationships derived from this data serve as an index for estimating the expected material properties and behavior when treating specific soil types under certain field conditions.

An initial bench study was conducted using a well graded sand (SW), in which the strength results were normalized for a rate of strength using Equation 2.1 to compare against data of different mixes and strengths. It was through this evaluation that it was found that soil type had a significant influence on the rate at which UCS increases in-situ due to curing stresses.

A total of three laboratory bench tests were conducted: one using a SW type soil as a base soil as part of a 2020 DFI research study, and two additional bench tests conducted in 2022/2023 in a subsequent study for DFI that included one using a high plasticity clay (CH) as the base soil and another study using a low plasticity silt (ML) as the base. Each of these bench studies were carried out using similar testing parameters that included classifying soil properties using Unified Soil Classification System (ASTM D 2487), preparation of soil-cement mixes in accordance with FHWA deep mixing manual (2013), assigning a binder factor and water-cement ratio (w:c) appropriate for the soil types being treated.

Bench test mix designs for each of these three bench studies included selection of a cement factor (α) and w:c ratio would typically be used in the field to treat these types of base soils. The cement factor is defined as the weight of the cement divided by the volume of the mixture (FHWA Manual, 2013). Typically, higher binder factors are required to treat finer grain soils. The binder type used for all these studies included standard Type I/II Portland cement. Municipal tap water was used as makeup water to prepare the mixes.

The values of the water-to-cement (w:c) ratio used in these bench studies ranged from 1.5 to 3.0. The w:c ratio plays a crucial role as a design parameter for deep mixing, as it not only influences the strength of the material but also determines the feasibility of treating a soil in the field. On a single project, the w:c ratio of a mix varies multiple times depending on the encountered soil conditions. In industry, a w:c ratio of less than 2.0 is generally preferred, as it helps mitigate the potential negative impact of excess water on material strength. However, when dealing with high plasticity clays, a w:c ratio greater than 2.0 is typically required to facilitate the mixing process.

The curing conditions selected for the bench tests are intended to simulate overburden pressures that a deep mixed materials would be subjected to in-situ. To evaluate the influence that curing stresses have on strength, specimens of the same batch must be subjected to a different curing stress. The testing framework reportedly used for the bench tests included preparing four test specimens of the same batch and subjecting each to a different curing stress and then testing for unconfined compressive strength after about 28 days of curing. Of the four specimens prepared; one specimen in each bench test was not subjected to an overburden pressure (σ_z = 0 psi) and was cured in a standard 3-inch by 6-inch plastic concrete test cylinder. The other three specimens were subjected to three increasingly higher stresses ranging from 6.0 to 8.8 psi, 12.0 to 17.7 psi, and 18.0 to 26.5 psi. Axial stresses are applied to the specimens using the modified field oedometer discussed in Section 3.1. Table 3.1 provides a summary of the testing parameters used in all three bench studies.

Once cured for about 28 days, unconfined compressive strength tests were then conducted on all four specimens in accordance with ASTM D 2166, Standard Test Method for Unconfined Compressive Strength of Cohesive Soil.

Table 3.1 Summary of Bench Test Parameters

Test Description	Base Soil Type (USCS)	Moisture Content (%)	Binder Rate a kg/m^3 (lbs./ft^3)	w:c ratio	Binder Type	Applied Curing Stress σ_z kPa (psi)
BT-1	SW	8	216.24 (13.5)	1.5	Type I/II Portland cement	0.0 (0.0) 60.7 (8.8) 122.0 (17.7) 182.7 (26.5)
BT-2	CH	58	291.47 (18.2)	3.0	Type I/II Portland cement	0.0 (0.0) 58.6 (8.5) 87.6 (12.7) 150.3 (21.8)
BT-3	ML	9.7	277.43 (17.32)	1.5	Type I/II Portland cement	0.0 (0.0) 41.4 (6) 82.7 (12) 124.1 (18)

Figures 3.2 and Figures 3.3 present the relationship of UCS values and overburden stress obtained for bench tests BT-2 and BT-3, respectively. Results for bench test BT-1 are shown in Figures 2.2 in Chapter 2.

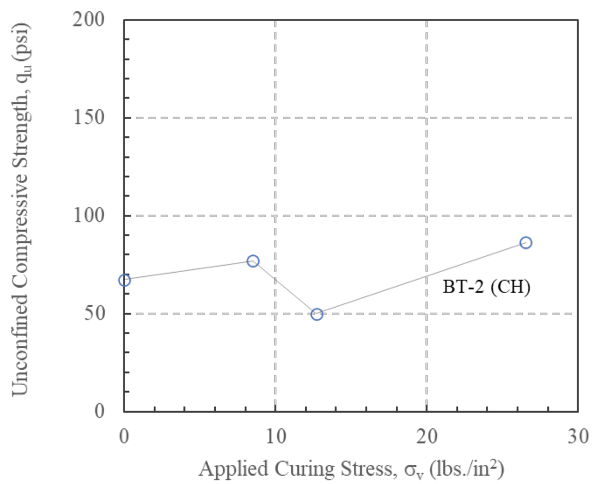

Figure 3.2 BT-2 (fat clay, CH) relationships between applied curing stress and UCS.

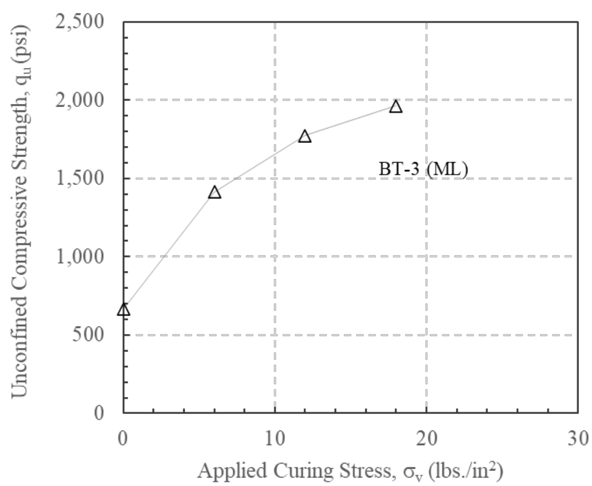

Figure 3.3 BT-2 (low plasticity silt, ML) relationships between applied curing stress and UCS

3.3 Bench Test Hydration Temperature Measurements

As part of the bench test 3 study, heat of hydration temperatures was also recorded from each of the test specimens prepared and cured in the laboratory. Temperatures were recorded by inserting insulated thermocouples through the bottom and into the center of each test specimen recording changes in temperature onto a datalogger while the specimens cured. Temperature recordings were continuous from the time the specimens were prepared up to the point that the specimens were taken down from the modified oedometer cells (21 days). Figure 3.4 shows a schematic of the testing setup.

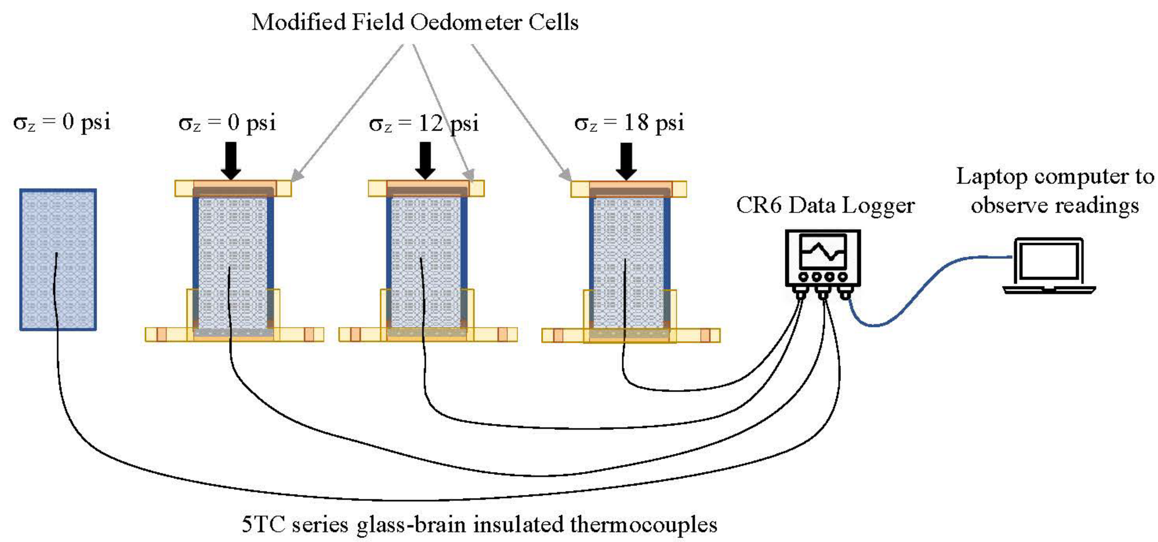

Figure 3.4 Schematic of BT-3 temperature recording setup.

Temperature data from this experiment was reportedly recorded for 496 hours, with a temperature reading being recorded every minute, totaling 26,769 temperature reading collected for each test specimen. Figure 3.5 shows the entire temperature data stream for all four specimens recorded. It's important to note that temperature oscillations observed beyond approximately 24 hours tend to exhibit a diurnal pattern due to changes in ambient temperatures in the laboratory.

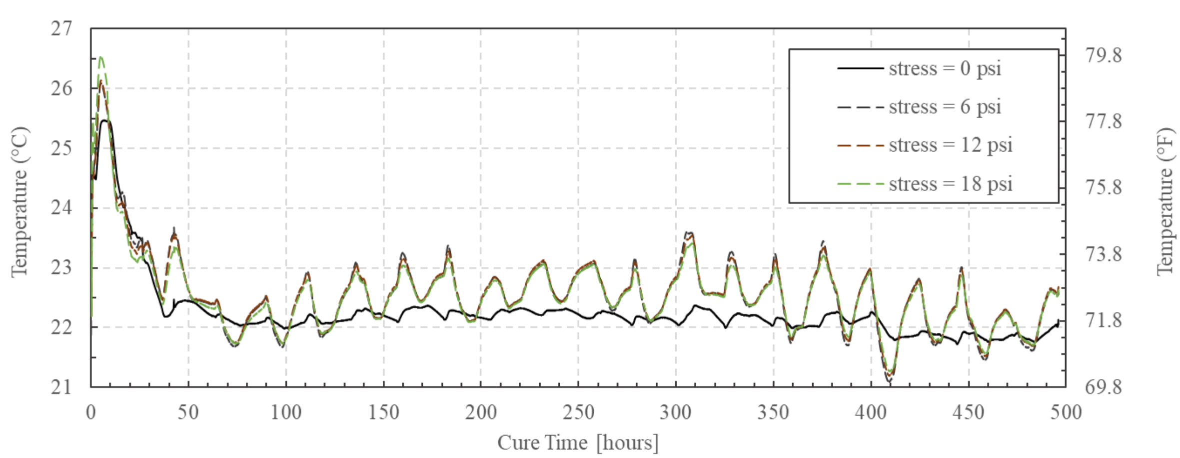

Figure 3.5 Hydration temperature data readings collected during curing of BT-3 test specimens.

3.4 Field Modified Oedometer Data

The approach of using field derived oedometer tests from active sites to study the influence of overburden stress during curing on cement-treated soil strength was pioneered by Onorato and Bonita with the objective of observing a broad range of soil types and mixing conditions from actual deep mixed sites so that in influence of overburden stress could be better quantified compared to data derived only through a laboratory study. To facilitate this approach, the modified oedometer apparatus (as described in Section 3.1) was set up at different field projects across the United Stated and Canada. It was only through the collaboration of several soil mixing contractors that valuable field data was able to be collected from a total of seven different projects.

The procedure for conducting the field modified oedometer test from an active field site was relatively consistent across all sites tested. The testing process involved first obtaining a bulk wet grab sample, weighing about 6 kilograms (kg), from a freshly mixed deep mixed column. This bulk sample is typically provided by the contractor as part of their quality control sampling program.

After collecting the bulk sample, four test specimens are prepared from it. These specimens consist of one that is molded within a typical 3-inch by 6-inch test cylinder and cured without any curing stress, and the other three specimens are loaded within the modified oedometers. The latter are cured under incremental increasing stresses, representing overburden pressures at various depths.

For each bulk sample data set, curing stresses generally range from 0 psi, 6 to 8 psi, 12 to 15 psi, and 20 to 30 psi. These applied curing stresses were kept relatively consistent across all sites tested. In addition, the procedures also record deformation and consolidation information during the curing period. All test specimens per data set are cured to the same during period, typically about 28 days before being tested for unconfined compressive strength using ASTM method 2166.

Preparations of the specimens were conducted in accordance with the specimen preparation procedures developed by Onorato and Bonita (2020), based on parametric study of different curing conditions. Figure 3.6 presents a photograph of a typical loaded field oedometer apparatus.

Figure 3.6 Loaded modified oedometer cell.

The field oedometer testing program collected data that included cement-treated soils with a range of well-graded sand and clayey sand (SW-SC), clayey-sand and low plasticity clay (SC-CL), clayey sand (SC), low plasticity clay (CL), and low plasticity silt and clay (CL-ML). This comprehensive dataset provided a broad range of grain size distributions, allowing for meaningful comparisons of strength data.

The data shown on Table 3.1 represent the data sets arranged only by the soil type that were, not by project site locations. The linear least squared value (R^2) of the *raw data* is also shown to present the linear correlation found within each dataset tested. The confidence levels of the linear fit correlations are indicated using the following guidance.

Very strong correlation ($R^2 > 0.75$)

Good to Strong correlation (R^2 0.5 < 0.75)

Poor correlation ($R^2 < 0.5$)

Due to the high variability of cement-treated natural soils, there are many non-confounding variables that could impact the correlations of these field results. To address this, a set of data validation criteria was established, and all datasets were required to meet these criteria before the results could be subjected to analysis. In general, validation of the data included screening out covariant, faulty tests, or incomplete datasets that could inadvertently cause a bias or could potentially skew or show a coincidence rather than a correlation within the datasets.

As a result of this validation standard, a considerable amount of acquired data was removed for not meeting the established validation criteria. See Section 4.0 *Data Validation Criteria* for more details regarding data validation criteria used for this study. The compiled list of validated data group collected from the field laboratory testing is presented in Table 3.2, which includes the soil type listed by the USCS classifications, the dry unit weight of the cured soil-cement material, γ_{dry} (lbs./ft^3) the void ratio recorded at the time of UCS testing, e, the unconfined compressive strength, q_u (lbs./in^2), the overburden curing stress, σ_v (lbs./in^2), and the R^2 value for the raw data set.

Table 3.2 Validated[1] Field Oedometer Data

USCS	γ_{dry} (lbs./ft^3)	e	q_u (lbs./in^2)	Curing stress σ_v (lbs./in^2)	Δq_u	Linear least squared fit of raw data (R^2)	
SC-CL	106	0.50	185	0	0	R^2 =	0.80
	108	0.46	309	9.0	0.7		
	123	0.17	305	18.0	0.7		
	116	0.39	652	27.0	2.5		
SC-CL	82.8	1.01	219	0	0	R^2 =	0.82
	91.6	0.82	495	8.6	1.3		
	93.7	0.79	518	17.3	1.4		
	96.3	0.72	596	25.9	1.7		
SC-CL	80.4	0.96	273	0	0	R^2 =	0.89

[1] Validated data indicates that the data met all the validation criteria described in Section 4.0

Table 3.2 Continued

USCS	γ_{dry} (lbs./ft^3)	e	q_u (lbs./in^2)	Curing stress σ_v (lbs./in^2)	Δq_u	Linear least squared fit of raw data (R^2)	
	99.2	0.67	288	4.7	0.1		
	91.1	0.79	574	10.9	1.1		
	92.1	0.75	584	14.0	1.1		
SC-CL	83.4	0.99	262	0	0	R^2 =	0.63
	95.3	0.72	535	8.7	1.0		
	99.6	0.67	559	17.5	1.1		
	102.0	0.59	549	26.2	1.1		
SW-SC	80.7	1.06	259	0	0	R^2 =	0.95
	93.2	0.78	400	11.7	0.5		
	99.1	0.67	541	23.4	1.1		
	99.6	0.66	580	35.0	1.2		
SC	87.5	0.91	296	0	0	R^2 =	0.62
	96.6	0.73	427	12.3	0.4		
	101.7	0.64	510	24.6	0.7		
	104.5	0.57	453	36.8	0.5		
SC	79	0.89	160	0	0	R^2 =	0.95
	88	0.88	254	9.0	0.6		
	89	0.83	316	14.2	1.0		
	91	0.90	360	24.1	1.3		
SC	85	0.90	277	0.0	0	R^2 =	0.92
	100	0.76	428	9.0	0.5		
	97	0.82	428	14.2	0.5		

Table 3.2 Continued

USCS	γ_{dry} (lbs./ft^3)	e	q_u (lbs./in^2)	Curing stress σ_v (lbs./in^2)	Δq_u	Linear least squared fit of raw data (R^2)
	98	0.89	518	24.1	0.9	
SC	76	0.91	167	0	0	$R^2 =$ 0.94
	86	0.92	292	8.99	0.8	
	88	1.03	303	14.15	0.8	
	87	0.89	380	24.05	1.3	
SC	79	0.92	126	0	0	$R^2 =$ 0.84
	84	0.83	241	9.0	0.9	
	83	0.89	213	14.2	0.7	
	86	0.82	294	24.1	1.3	
SC	77	0.92	170	0	0	$R^2 =$ 0.77
	86	0.96	326	9.0	0.9	
	89	0.89	296	14.2	0.7	
	89	0.89	361	24.1	1.1	
SC	74	0.93	173	0	0	$R^2 =$ 0.64
	85	0.80	264	9.0	0.5	
	83	0.82	226	14.2	0.3	
	84	0.89	273	24.1	0.6	
SC	75	0.92	212	0	0	$R^2 =$ 0.88
	84	0.90	348	9.0	0.6	
	84	0.93	355	14.2	0.7	
	85	0.98	410	24.05	0.9	

Table 3.2 Continued

USCS	γ_{dry} (lbs./ft^3)	e	q_u (lbs./in^2)	Curing stress σ_v (lbs./in^2)	Δq_u	Linear least squared fit of raw data (R^2)
CL	76.3	1.15	208	0	0	R^2 = 0.53
	87.5	0.88	481	4.4	1.3	
	93.0	0.78	542	10.9	1.6	
	90.8	0.83	454	14.0	1.2	
CL-ML	84.1	0.93	156	0	0	R^2 = 0.97
	93.6	0.73	409	6.0	1.6	
	97.7	0.63	503	12.0	2.2	
	100.0	0.61	699	18.0	3.5	
CL-ML	92	0.74	91	0	0	R^2 = 0.86
	93	0.75	106	9.0	0.2	
	102	0.63	404	18.0	3.4	
	100	0.74	439	27.0	3.8	
CL	81	0.91	213	0	0	R^2 = 0.91
	92	0.89	505	9.0	1.4	
	93	0.98	624	14.2	1.9	
	96	1.06	706	24.1	2.3	
SW-SC	102	0.67	590	0	0	R^2 = 0.94
	105	0.51	740	8.99	0.3	
	108	0.45	793	14.15	0.3	
	107	0.47	856	24.05	0.5	

3.5 In-situ Stress and Temperature Measurements

To investigate the internal stresses within a freshly mixed deep mixed column, an in-situ field instrumentation testing program was initiated that measures total lateral stress using push-in pressure cells installed vertically near the center of a deep mixed column. A distinct vibrating wire piezometer was necessary for measuring pore pressures. Unfortunately, due to time limitations on the project, the instrument could not be installed.

The main objective of the in-situ instrumentation program was to observe changes in in-situ total and effective lateral stresses and curing temperatures shortly after the deep mixed column was created. The in-situ testing program mainly focused on stresses and temperature changes within the first 24 hours of being mixed, however, data was available up to about 68 hours providing valuable insight on changes that occur within this curing period. The collection of this data included utilization of a vibrating wire push-in pressure cell (model 4830-1-350KPA) manufactured by GEOKON that was provided specifically for the DFI research.

Figure 3.7 depicts a photograph of the pressure cell instrumentation employed. It's worth noting that the pressure cell records stresses that are perpendicular to the flat surface. Consequently, when the pressure cell is installed vertically, it measures horizontal stresses.

Figure 3.7 GEOKON Model 4830 Push-in Pressure Cell

The initial field project from which in-situ measurements were collected was a ground improvement endeavor situated in the coastal region of Southern Louisiana. Soil's being treated for this site primarily consisted of low plasticity clay and silt (CL-ML), and the method of deep mixing was a specialized mixing tool known as cutter soil mixing (CSM). Unlike traditional deep mixed cylindrical columns, the CSM creates a rectangular shaped panel that measures about 1 meter in width by 2.8 meter in length.

The instrumentation test was conducted in late 2019. The pressure cell instrumentation started recording stresses and temperature readings approximately 90 minutes after the CSM panel was created and continued for 20.3 hours. The pressure cell was installed about 16.95 feet into the CSM panel, and data began recording as soon as the instrumentation was installed. The water table at the site was approximately 3 feet below ground surface. Both horizontal stress (P_h) and temperature (T) data were recorded at 15 second intervals. The P_h data is shown in pound per square foot (lbs./ft^2). The temperature was recorded directly in degree Celsius. Figure 3.8 shows P_h-data and T-data versus time post mixing collected during the event.

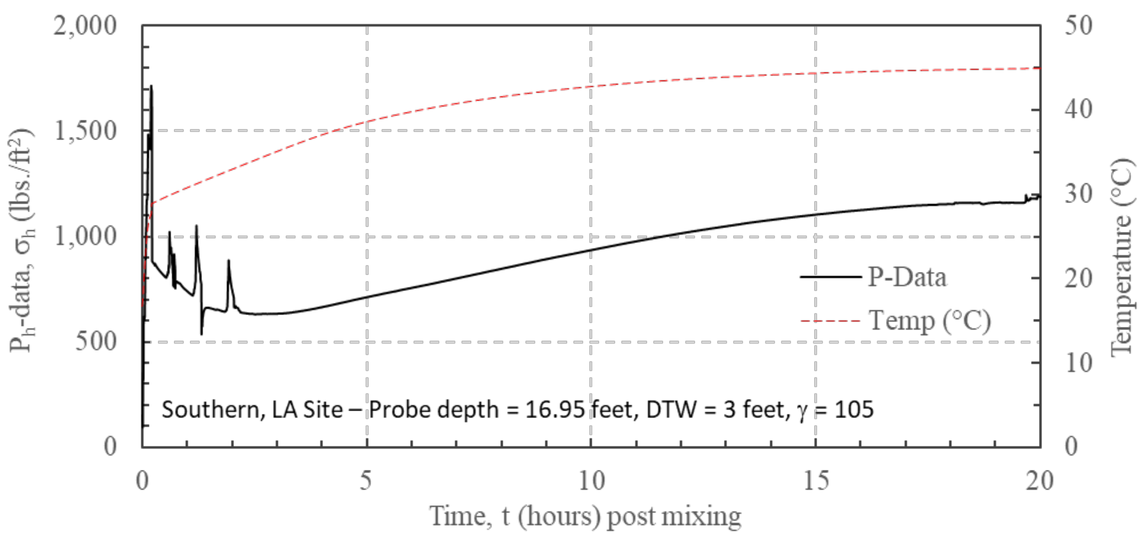

Figure 3.8 Site 1 in-situ lateral stresses (P_h-data) and temperature readings versus time post mixing.

In-situ instrumentation data was also collected at a second site located in central Colorado in mid-2020, following a similar methodology as the first site. The soils treated at this second site primarily consisted of silty and clayey sand (SC-SM), and the deep mixing method was performed using a traditional 8-foot diameter auger.

The same type of push-in pressure cell instrument (model 4830-1-350KPA manufactured by GEOKON) was used to collect data and it was reported that data began approximately 48 minutes after the deep mixed column was mixed and the data continued for 67.9 hours post mixing. P_h-data and temperature readings were recorded every 15 seconds. The push-in pressure cell was installed about 16 feet into the deep mixed column. The water table at the site was reported to be about 7.5 feet below ground surface.

Figure 3.9 shows the P_h-data (horizontal stress) and temperature versus time, t post mixing recorded during the test event. For comparison, only the first 20 hours of the data stream are shown in the figure.

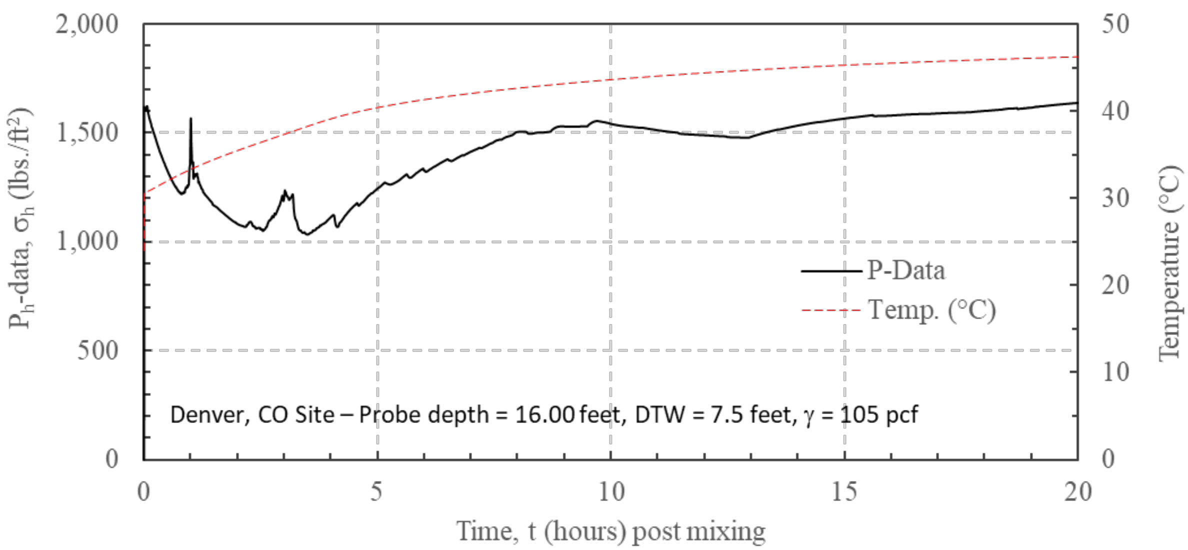

Figure 3.9 Site 2 in-situ lateral stresses (P_h-data) and temperature readings versus time post mixing.

3.6 Deep Mixed Core Run Strength Data

The core run data obtained from a selection of deep mixed projects was used to compare against the empirical data derived from bench tests and field oedometer test results. Core run testing at deep mixed sites is a commonly employed method for quality control in various cement-treated soil applications. The process of coring a deep mixed soil-cement column resembles coring drilling in weak bedrock for geotechnical assessments. While this data typically provides satisfactory results, it is crucial to recognize that, in certain cases and ground conditions, the drilling process can damage the specimens, potentially leading to a misrepresentation of their actual in-situ strength. Therefore, when using core data for research purposes, these potential flaws must be addressed.

Furthermore, there are several factors to consider regarding deep mixed materials that affect the core run results. Factors such as variations in material consistency, soil types, and installation deviations can affect the results. As a result, core run data from deep mixed sites may not serve as an ideal analog from a material mechanics perspective when compared to materials tested from the same batch mix. However, despite possible inconsistencies within the datasets, it is believed that general strength-gaining behavior trends may still exist, allowing for comparisons with laboratory and field oedometer data.

To address the potential issues with the coring data, a data validation process described in Section 4.0 was employed to screen out non-conforming conditions, making the coring data reasonably comparable to the data presented in this study.

Various sources of variability need to be considered when utilizing coring data for this study. These include geologic variability within the deep mixed column, operational variability, such as differences in deep mixed injection parameters (e.g., binder rates and water-to-cement ratios), and specimen quality variability. Specimen quality variability can involve the presence of unmixed clods, voids within the specimens, the presence of aggregates/shells, or damages to the specimens that may have occurred during drilling, as discussed in this section.

Using the data validation criteria described in Section 4.0, data sets which contained non-representative conditions were removed from the final core data group. Details regarding the tools and data validation criteria used in this program are described in Section 4.0 *Data Validation Criteria.*

Table 3.3 presents the entire validated coring dataset identified by the USCS soil type that was treated, the calculated overburden stresses, σ_v and the rate of stress change, Δq_u at each stress interval. Due to confidentiality agreements with the collaborators that provided the coring data, actual unconfined compressive strength, q_u values are omitted. The linear squared fit value (R^2) of the *raw data* is also shown to present the natural correlation found between material strength (UCS) and overburden stress within each dataset. The strengths of the correlations between curing stress and material strength exhibited within this data group are represented using the following guidance shown below.

Very strong correlation ($R^2 > 0.75$)

Good to Strong correlation (R^2 $0.5 < 0.75$)

Poor correlation ($R^2 < 0.5$)

Table 3.3 Validated Core Data Group

USCS	Curing stress σ_v (lbs./in^2)	Δq_u	Linear least squared fit of raw data[2] (R^2)
SC-CL	0	0	$R^2 =$ 0.89
	5.7	0.4	
	11.4	0.7	
	19.4	1.9	
	27.3	1.8	
	31.8	2.2	
CL-ML	0	0	$R^2 =$ 0.92
	6.9	1.2	
	13.9	1.6	
	21.5	3.3	
	29.8	7.3	
	32.3	7.1	

[2] Raw Data Fit is defined as the unnormalized correlation between actual UCS values and overburden stress.

Table 3.3 Continued

USCS	Curing stress σ_v (lbs./in^2)	Δq_u	Linear least squared fit of raw data (R^2)
CL-ML	0	0	$R^2 =$ 0.97
	7.6	0.4	
	12.2	1.2	
	18.4	2.6	
	25.2	3.2	
	34.3	6.2	
CL-ML	0	0	$R^2 =$ 0.96
	7.3	1.0	
	15.3	1.5	
	22.6	3.0	
	28.6	4.4	
	34.4	4.9	
SC	0	0	$R^2 =$ 0.82
	3.8	0.3	
	8.2	0.1	
	9.2	0.3	
	14.2	0.3	
	19.0	0.6	
	27.6	1.2	
SC-CL	0.0	0	$R^2 =$ 0.98
	4.6	0.3	
	8.6	0.4	

Table 3.3 Continued

USCS	Curing stress σ_v (lbs./in^2)	Δq_u	Linear least squared fit of raw data (R^2)
	14.7	0.9	
	27.9	2.0	
SC-CL	0	0	$R^2 =$ 0.46
	2.7	0.1	
	7.2	1.1	
	15.9	1.4	
	21.3	1.2	
	31.4	1.2	
CL	0	0	$R^2 =$ 0.62
	6.3	0.7	
	14.5	0.3	
	18.8	0.9	
	26.8	4.6	
	32.3	3.1	
CL-ML	0	0	$R^2 =$ 0.90
	16.7	0.2	
	20.6	-0.2	
	26.0	2.2	
	30.9	4.0	
	34.5	7.0	
SC	0	0	$R^2 =$ 0.74
	3.8	0.2	
	11.5	0.2	

Table 3.3 Continued

USCS	Curing stress σ_v (lbs./in^2)	Δq_u	Linear least squared fit of raw data (R^2)
	18.1	0.2	
	30.0	2.0	
CL	0	0	$R^2 =$ 0.52
	3.2	0.8	
	7.6	0.6	
	9.1	0.9	
	11.7	1.4	
	12.4	1.2	
CL	0	0	$R^2 =$ 0.75
	12.9	1.1	
	16.4	1.3	
	17.0	1.1	
	24.5	1.5	
	32.1	2.6	
	32.8	2.0	
	37.8	4.3	
CL-ML	0	0	$R^2 =$ 0.92
	6.4	0.1	
	12.8	1.7	
	15.2	3.1	
	19.2	3.3	
CL-ML	0	0	$R^2 =$ 0.44
	12.8	0.7	

Table 3.3 Continued

USCS	Curing stress σ_v (lbs./in^2)	Δq_u	Linear least squared fit of raw data (R^2)
	15.2	4.2	
	17.6	3.8	
	19.2	3.4	
SC	0	0	$R^2 =$ 0.59
	11.9	0.3	
	14.8	0.3	
	18.2	0.3	
	25.2	0.9	
	28.3	0.1	
	33.8	1.5	
	37.5	3.0	
SC	0	0	$R^2 =$ 0.69
	16.4	0.7	
	21.3	0.8	
	25.4	0.6	
	29.1	1.0	
	32.8	2.4	
	36.9	2.6	
CL	0	0	$R^2 =$ 0.79
	14.1	1.5	
	18.9	2.1	
	22.5	1.7	
	26.2	2.4	
	31.1	3.9	
	35.2	6.3	

Table 3.3 Continued

USCS	Curing stress σ_v (lbs./in^2)	Δq_u	Linear least squared fit of raw data (R^2)
CL	0	0	R^2 = 0.89
	10.2	0.4	
	15.1	1.9	
	19.6	1.3	
	23.6	2.6	
	27.6	3.3	
	31.7	3.2	
	35.8	4.9	
SW-SC	0	0.0	
	8.6	0.0	R^2 = 0.68
	12.7	-0.1	
	16.8	0.2	
	20.9	0.1	
	25.0	0.4	
	29.1	0.3	
	33.2	0.9	
	44.7	0.7	
SC	0	0.0	R^2 = 0.76
	12.7	0.4	
	16.8	0.3	
	20.9	0.6	
	29.1	1.1	
	33.2	0.8	
	37.3	1.8	

Table 3.3 Continued

USCS	Curing stress σ_v (lbs./in^2)	Δq_u	Linear least squared fit of raw data (R^2)
SC-CL	0	0	$R^2 =$ 0.86
	7.7	0.2	
	11.4	0.9	
	15.0	1.3	
	15.9	0.6	
	22.8	1.5	
	28.4	2.6	

CHAPTER 4
DATA VALIDATION CRITERIA

The data validation program had a primary objective of verifying the alignment of values in each dataset with acceptable criteria from a material consistency standpoint. Additionally, it aimed to ensure that the independent variables covered a wide range and sufficient quantity to minimize the likelihood of coincidental correlations within the dataset, emphasizing meaningful connections. The ultimate aim of data validation was to ensure a certain level of quality for the comprehensive database.

This data validation program was built upon a decisional procedure consisting of meticulously crafted rules, designed to identify nonconformities like defects, sampling errors, or testing inaccuracies. These nonconformities could potentially influence material properties leading to inconclusive correlations. The groundwork for this validation framework was laid by Daas et al. (2011), who formulated rules based on statistical consistency and the impact of specific variables on the overall results. These rules were then applied to the data to determine its eligibility for inclusion in the dataset. Data satisfying these rules was considered valid and eligible for further analysis.

A strict data validation program was absolutely critical for this project, given the inherent variability present in deep mixed materials from one location to another. Ground conditions, operational deviations during production, and material inclusions like unmixed clay, rocks, or shells significantly impacted strength values. Due to these complexities, most academic research on deep mixed materials was conducted on laboratory-prepared materials with known soil and admixture properties rather than taking into consideration the variability of actual field conditions. While this information could be valuable for understanding general engineering properties and behavior under specific conditions, it might not always be directly applicable to real-world scenarios.

4.1 Validation Rules

A comprehensive system was derived comprising of three distinct levels of validation rules, each tailored to the specific tier or analysis being conducted. The purpose of these validation levels and rules was to identify and filter out erroneous, inconsistent, or non-representative data from the datasets. The assignment of validation levels was based on the influence that each variable could exert within the data group.

In the data validation program a multi-tiered approach was employed to scrutinize the dataset thoroughly. At level 0, a comprehensive assessment was conducted to ensure the dataset's overall consistency and integrity. This initial stage aimed to identify any potential anomalies or discrepancies that could impact the entire dataset.

Subsequently, the analysis progressed to levels 1 and 2, where a more granular examination took place, focusing on specific subsets of data. Here, the goal was to explore the consistency of individual components within these subsets and investigate their interrelationships. This deeper level of scrutiny aimed to uncover any localized variations or irregularities that might not be apparent at the higher level of analysis.

By adopting this tiered approach, the system aimed to enhance the reliability and accuracy of the data. The process involved filtering out any data points that exhibited inconsistencies or appeared to deviate significantly from the expected patterns, thus minimizing the potential for distorting the overall analysis and ensuring the dataset's robustness for further research and conclusions. Level 0 validation rules apply to all acquired datasets. Level 1 validation rules apply to data that have met all the level 0 validation rules but are datasets used for trend analysis. Level 2 validation rules apply only to the extrapolation of specific data points required for analysis; and only applies to datasets that have met all the criteria of Level 0.

The primary purpose of the first level of validations (Level 0) is to eliminate any conditions that could lead to unrepresentative values in the dataset. It also ensures that the sample size is sufficiently large to reduce the likelihood of coincidental occurrences within the data. By performing these checks, the validation process aims to establish a more accurate and reliable representation of the underlying data. Level 0 rules include are described in Table 4.1.

Table 4.1 Level 0 Validation Criteria

Rule number	Level 0 Rules	Description
1	Minimum Dataset Size	A complete dataset must include at least four consecutive data points.
2	Overburden Stress Range	The minimum range between the first and last data value must represent a depth range of at least 10 feet (or 7 psi).
3	Outlier Removal	Outliers may be removed if criteria (1) and (2) are met.
4	Exclusion Criteria	Data from test specimens with recorded unmixed clods, voids, or shells are excluded.
5	Binder Rate Consistency	The binder rate and water-to-cement ratio must be consistent within the entire dataset.
6	Soil Type Consistency	The soil type must be relatively consistent within the entire dataset.

At the Level 1 data validation stage, the objective is to enhance the precision of data trends without introducing substantial alterations to the overall results. This refinement process involves cross-referencing the observed strength gain for specific soil types with data obtained from two additional sources: the bench test and the laboratory field oedometer data, and/or coring testing results data.

By selectively removing lower fit datasets, the goal is to "tighten" the range of data points, resulting in a more precise correlation. Table 4.2 outlines the level 1 validation criteria that must be met before data is evaluated. This step contributes to improving the reliability and accuracy of the findings without significantly influencing the overall outcome of the analysis. It allows for a more nuanced understanding of the strength gain patterns and the interrelationships between different soil types, enhancing the validity of the conclusions drawn from the research. Before Level 1 rules are applied to any dataset, Level 0 criteria must be met.

Table 4.2 Level 1 Validation Criteria

Rule number	Level 1 Rules	Description
1	Qualified Dataset	Data must meet all Level 0 validation criteria
2	Correlation strength	Raw or un-normalized dataset must have minimum least squared linear fit (R^2) of 0.80 of higher.
3	Dataset correlation	Raw or un-normalized dataset trends must not contain any extrapolated or data fitted points.

At Level 2 data validation, the focus is solely on core run datasets that lack unconfined compressive strength data for a specific condition where no overburden stress was tested. In such cases, this datapoint is used solely to extend the linear correlation line to predict strength without the influence of overburden stress.

The primary goal here is to ensure that the inclusion of this datapoint does not have a significant impact on the slope of the strength gained when including the fitted value. By carefully considering this extension, the hopes were to maintain the integrity of the strength gain data trend while accounting for the absence of overburden stress data to develop an empirical relationship from that point. This validation process is essential to avoid any distortion in the overall correlation and to ensure the accurate representation of strength gained in the absence of relevant testing conditions.

Table 4.3 Level 2 Validation Criteria

Rule number	Level 1 Rules	Description
1	Qualified Dataset	Data must meet all Level 0 validation criteria
2	Qualified Data Points	When fitted values are used to complete a coring dataset, the UCS value with no overburden stress must be within one standard deviation of the average wet grab UCS strength for that entire dataset, if available.
3	Qualified correlation guideline	The best linear square fit (R^2) for a dataset using a fitted data point cannot be higher than the unnormalized linear fit without the fitted data point.

4.2 Data Fitting

Data fitting serves as a valuable tool to refine correlations within specific datasets, enabling the combination of research data from various sources into a unified model. In this study, data fitting is employed solely to extrapolate an estimated unconfined compressive strength value at a curing stress of zero ($q_{u,0}$). This application is particularly relevant to the collected coring run data, where strength values were provided at specific depths within the column, but UCS values for specimens cured without confinement are typically missing.

To be considered for inclusion, all fitted datasets must meet the stringent data validation criteria for Level 0 without any fitted data being incorporated initially. Any dataset failing to satisfy the Level 0 data validation requirements was excluded from the entire data group.

To accomplish the fitting of $q_{u,0}$, a residual sum of squares (RSS) method with the objective of establishing the best linear fit between the dataset with the predicted $q_{u,0}$ data point and the dataset without this datapoint. The fit is further assessed using the RSS, R^2 value, and slope of the regression lines. Equation 4.1 represents the RSS calculation:

$$RSS = \sum_{z=1}^{n} \left(q_{u,z} - \widehat{\beta_o} - \widehat{\beta_1}\sigma_z\right)^2 \quad (4.1)$$

Where, $\widehat{\beta_0}$ is the estimated $q_{u,0}$ value (psi) and $\widehat{\beta_1}$ is the slope of regression line of the unnormalized dataset, σ_z is the confinement stress at a depth z (psi), and $q_{u,z}$ is the measured UCS value from the coring data at depth z (psi).

This approach allows for the estimation of $q_{u,0}$ values, enhancing the completeness and applicability of the dataset for further analysis and modeling.

CHAPTER 5
RESULTS AND DISCUSSION

This chapter evaluates the data and discusses the influence of overburden curing stress on the strength of deep soil mix materials. The initial section discusses the parameter (Δq_u) defined by Equation 2.1 used to normalize the datasets, allowing for an equal comparison of the influence of overburden stress across all data sources. Next, the results of the data are evaluated from the three primary sources, each of which is discussed in the following order: laboratory prepared bench tests, field oedometer testing using materials from a deep mixed site, and strength data obtained from soil mix cores conducted on active deep soil mix projects.

After the main body of data and analyses, the subsequent section evaluates the results of two in-situ pressure cell tests conducted at active deep mixed sites. Furthermore, the last two sections present and discuss related analyses that compare the recorded heat of hydration from the in-situ tests with the heat of hydration collected from bench test specimens cured at ambient laboratory temperatures.

Concluding this chapter, a desktop evaluation examines the effects of water-to-cement ratio on UCS (unconfined compressive strength) results, both from actual data and empirical relationships. Additionally, it includes a comparison of the rate of strength change (Δq_u) observed from the effective water-to-cement differences calculated within the consolidated specimens presented alongside the bench studies conducted as part of this study.

5.1 Rate of Strength Change (Δq_u)

The parameter of rate of change, Δq_u (Equation 2.1) is a crucial measure used to assess the influence of overburden stress on deep soil mix material strength across different soil types and different binder rates. It represents the change in unconfined compressive strength (UCS) under different curing stresses. It is further theorized that the slope of this rate of strength change is influenced by the specific base soil types that are being treated. The parameter Δq_u has been instrumental at identifying the key dependent variables that influence strength gains of cement-treated soils produced via deep mixing.

The meaning of Δq_u as it related to this study lies in its ability to quantify the relative strength difference across the different data sources reviewed for this study. By comparing the slope of UCS rate of change under various curing conditions and across different data sources, this data reveals insights into how both overburden stresses and different soil types influence in-situ strength.

The purpose of Δq_u is comprehensive, and include:

Evaluating the Influence of Curing Stress: Δq_u allows assessment of how overburden curing stress influences the strength properties of deep soil mix materials in-situ. It helps to identify whether material properties significantly affect the changes in strength when subjected to varying degrees of in-situ confinement, providing insights into material behavior under different conditions.

Normalization and Comparison: By normalizing the datasets using Δq_u, Onorato and Bonita standardized the comparison of UCS values from different sources. It ensures a fair comparison between laboratory prepared bench tests, field oedometer testing, and strength data obtained from soil mix cores, enabling a comprehensive analysis across various data sets.

Evaluating Material Performance: The rate of change parameter is an essential tool to assess the expected performance and suitability of deep soil mix materials for specific engineering applications. It aids in identifying the ideal conditions for optimal material strength, which can inform design considerations for ground improvement applications.

Empirical estimations of in-situ strengths: The parameter of Δq_u also facilitates an empirical relationship between overburden curing stress and soil types so that a UCS value could be estimated based only on a wet grab specimen that was cured without overburden stress.

Overall, Δq_u is an integral parameter in deep soil mix research, offering valuable insights into the material's strength characteristics under varying curing conditions. It enables engineers to make informed decisions regarding the estimated in-situ strength when actual strength data is not readily available or easily obtained. Having insight into the empirical estimated of in-situ strength also assists engineers with the evaluation of quality control data on a project.

5.2 Laboratory Bench Testing Results

This section discussed the relationships uncovered from the results of several bench tests conducted as part of the study. The first bench test was conducted using a well graded sand (SW) as a base soil which showed a relatively modest strength gain relationship. Having only limited information, this result only demonstrated that curing stress indeed had an influence on the strength of the mix. It wasn't until a broader range of data was evaluated using a variety of soil types that it became apparent that soil type or more specifically grain size may also have an influence on the rate of which strength gains in-situ.

Using other data sources including field oedometer testing and core run data, it was concluded semi-quantitatively that the treatment fine-grans soils demonstrated higher strength gains than granular soil. It is recognized, however, that the relationship of strength gains and soil types were based solely on just observations of all normalized field data, which could present some degree of inconsistency due to material variances of this type of unvalidated field data.

To better measure these observations, two additional controlled laboratory bench tests used fine grain soils to quantify the preliminary findings. A controlled bench study eliminates the many inconsistencies that would normally be present in actual field work. The second bench study conducted in 2020 consisted of a high plasticity clay (CH) at the base soil type; this bench test was referred to as "BT-2".

Reports during the testing process provided valuable insight into the behavior of cement-treated mix that included high plasticity clay as curing loading was applied. It was reported that during the loading of the oedometer cell, consolidation of the specimens ceased within a few minutes, and that both the upper and lower porous stones had clogged, thereby ceasing drainage out of the specimens. This information provided important insight into the limitations that high plastic clays have in short-term consolidation and helped to understand the role that drainage and consolidation have on strength gain. Table 5.1 presents important parameters, strength changes, and volumetric information from BT-2 that is considered for evaluation of the bench test.

Table 5.1 Summary of BT-2 strength, density, and volumetric data

Dry Density kN/m^3 (lbs./ft^3)	Void ratio* e	UCS q_u kPa (lbs./in^2)	Applied Curing Stress σ_v kPa (lbs./in^2)	Rate of Change Δq_u	Height of specimen, H cm (in)
9.0 (57.4)	1.88	464 (67.4)	0 (0.0)	0.01	15.19 (5.98)
8.4 (53.3)	2.10	530 (76.9)	59 (8.5)	0.14	14.10 (5.55)
8.6 (54.8)	2.02	345 (50.0)	88 (12.7)	-0.26	14.91 (5.87)
8.0 (50.8)	2.26	595 (86.4)	183 (26.5)	0.28	14.96 (5.89)

*Void ratios were estimated using Equation 5.1 (*Das, B., 1941*)

$$e = \frac{G_s \gamma_w}{\gamma_{dry}} - 1 \tag{5.1}$$

Where, G_s is the specific gravity of the base soil (2.65), γ_{dry} is the dry unit weight of the soil-cement specimen, and γ_w is the unit weight of water (62.4 lbs./ft^3).

The results in Table 5.1 show that consolidation of the specimens ceased very early on the loading process and that material properties were irregular. Consequently, the strength results show no significant correlation with either applied curing stress, and interestingly nor was there a relationship between strength and the amount of consolidation (height of the specimens) as well. This appears to be an indication that the material is not draining; therefore, not consolidating.

Figure 5.1 shows the relationship of overburden curing stress (σ_v) to the rate of strength increase (Δq_u), again showing no significant correlation.

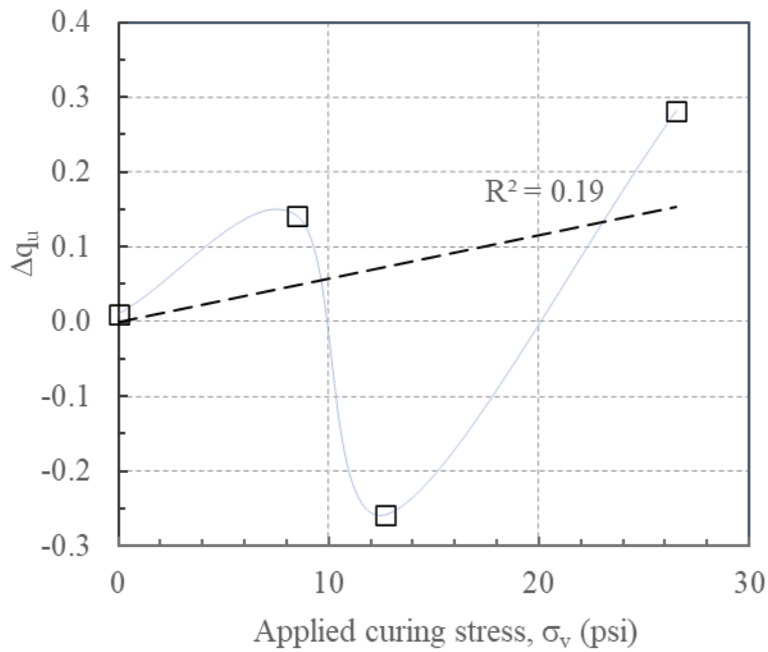

Figure 5.1 BT-2 relationship of applied curing stress, σ_v to the rate of change in unconfined compressive strength, Δq_u

The bench test results are interesting, showing similarities with most evaluated coring sample runs involving high plasticity clays treatment. The linear square fit for this dataset has a low R^2 value of less than 0.20, indicating limited confidence in strength dependence on confinement stress during curing.

Poor-quality intermixing of grout within the soil matrix contributes to lower and less predictable strength gains. Despite efforts to achieve thorough mixing, hydrophobic properties of plasticity clays hinder complete intermixing, resulting in a heterogeneous composition. Figure 5.2 shows a conceptual illustration of a typical high plastic clay-cement material composition.

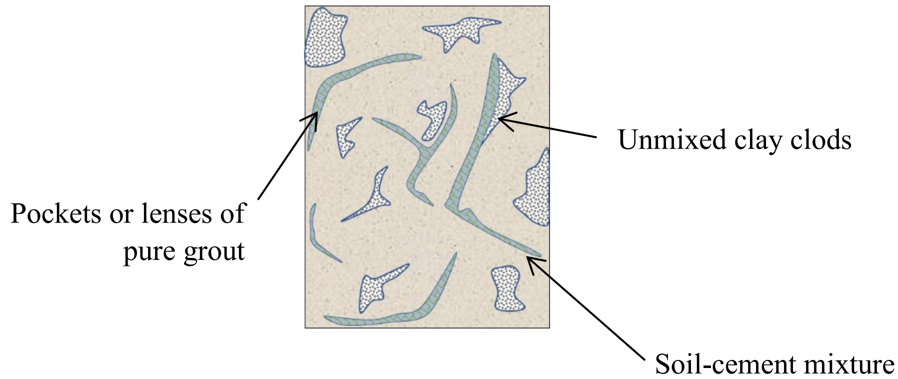

Figure 5.2 Illustration of a typical mix heterogeneousness with highly plastic clays.

As illustrated in Figure 5.2, soil-cement mixtures commonly exhibit a heterogeneous composition when mixing plastic clays, resulting in the presence of unmixed clods seen both in wet grab samples and within core run specimens. Moreover, the composition of the material may contain aggregates, voids, or pockets of porewater, all of which can influence the unconfined compressive strength (UCS) values of tested specimens. This condition presents great challenges to engineers attempting to evaluate the strength and mechanical properties of these materials in-situ.

Another significant factor contributing to the limited strength gains in this scenario is the low permeability of plastic clay. During the early stages of curing, drainage and consolidation are hindered, limiting interparticle contact (adhesion). Consequently, the material's ability to gain strength with confinement pressure during curing is restricted. These combined factors underscore the challenges in achieving substantial strength improvements for soil-cement mixtures involving plastic clays.

To gain a better understanding of the strength gain behavior of cement-treated fine-grain soils, particular to the observations seen within the field oedometer and core run data, a third controlled laboratory bench test using a low plasticity fine-grain (ML) soil as the base soil type. This specific bench test was referenced as BT-3.

The purpose of BT-3 was to provide additional insights into the strength development of cement-treated fine-grain soils and to complement the findings from the other data sources. By conducting a controlled laboratory test, the aimed was to compare the results against the observed strength behaviors seen in the field oedometer and core run data.

Upon analyzing the results of BT-3, a linear strength gain was observed. This data aligned with the other observed data sources, reinforcing the reliability and consistency of the overall findings.

Table 5.2 presents key information, including the rate of strength changes, density measurements, and volumetric data obtained from BT-3. These parameters provide valuable insights into the strength development mechanisms that are occurring during the curing process under stress.

By combining the results from the field oedometer, core run data, and the bench test BT-3, the study gains a more comprehensive understanding of how cement-treated fine-grain soils respond to various curing stresses.

Table 5.2 Summary of BT-3 strength, density, and volumetric data

Dry Density kN/m^3 ($lbs./ft^3$)	Void ratio* e	UCS q_u MPa ($lbs./in^2$)	Applied Curing Stress σ_z kPa ($lbs./in^2$)	Rate of Change Δq_u	Height of specimen, H cm (in)
15.7 (100.1)	0.65	4.58 (665)	0 (0)	0	15.09 (5.94)
16.9 (107.3)	0.54	9.74 (1,415)	41 (6)	1.13	14.12 (5.56)
17.4 (110.5)	0.50	12.23 (1,775)	83 (12)	1.67	13.92 (5.48)
17.6 (112.2)	0.47	13.53 (1,965)	124 (18)	1.95	13.18 (5.19)

*Void ratios were estimated using Equation 5.1.

Figure 5.3 shows a key relationship between applied overburden stress (σ_z) to the rate of strength increase (Δq_u) for the low plasticity clay soils, which are dramatically different than the results using high plastic clays. The results show a consistent trend in density increases and void ratio reduction as would be expected with consolidation.

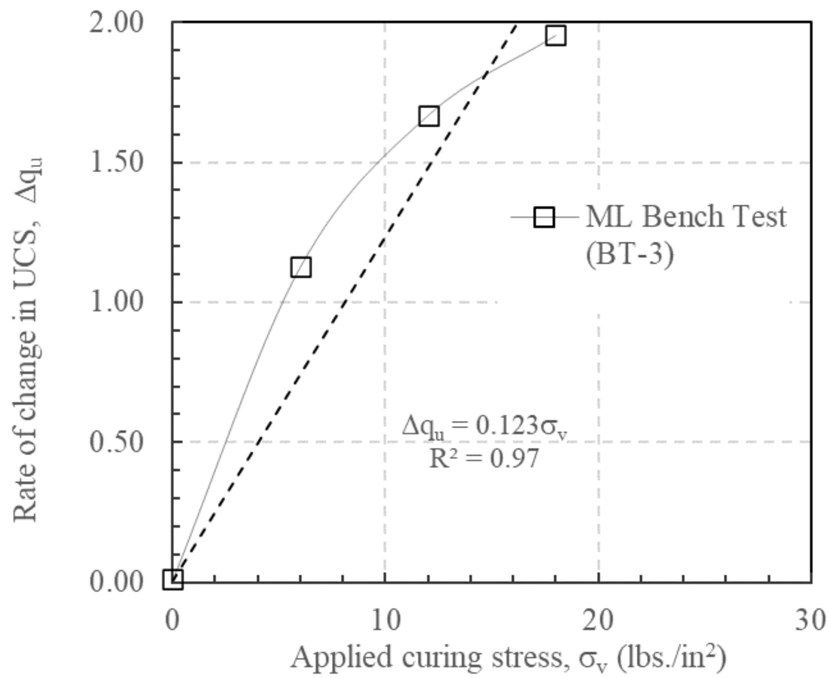

Figure 5.3 BT-3 relationship of applied curing stress, σ_v to the rate of change in unconfined compressive strength, Δq_u.

A comparison of the laboratory bench test results shows that strength gains were influenced by curing stresses and soil type (or more specifically grain sizes) have an influence on the rate at which strength is gained. The results showed that fine grain soils had a greater rate of strength gain than granular soil. An exception to these trends in strength gain being observed appears to be with high plasticity clays which do not appear to show strength gain. This is likely due to the low permeability of the clay and the lack of drainage and consolidation. Figure 5.4 presents a comparison of the rate of strength gains, Δq_u for both the granular bench test (BT-1) and the fine grain soil bench test (BT-3).

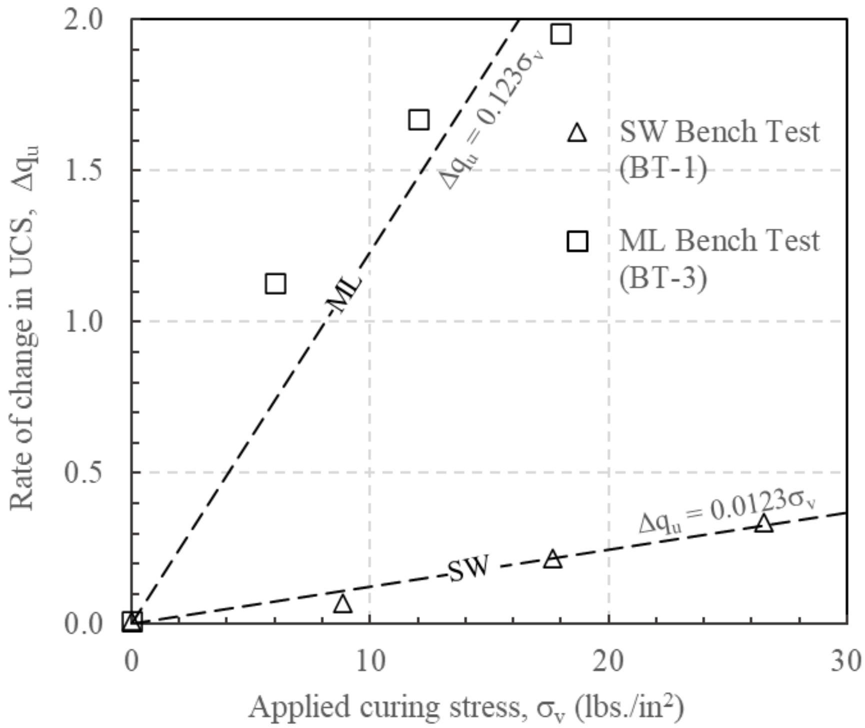

Figure 5.4 Comparison of Δqu for BT-1 (SW) and BT-3 (ML)

The comparison of volumetric changes in specimen height (Δh) to the applied curing stress between BT-1 and BT-3 offers valuable insights into the drainage and consolidation behavior during the curing process when a curing stress is applied. Figure 5.5 shows the relationship of Δh and applied stresses during the curing process.

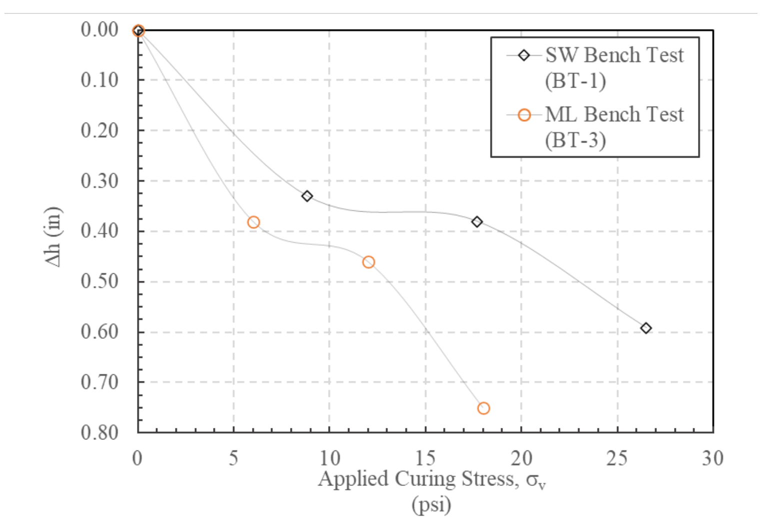

Figure 5.5 Relationship between Δh and applied curing stress for SW and ML soil types.

By comparing these results, the specimen with finer grain particles (ML) exhibits greater volume change per applied curing pressure, which is expected given that a greater void ratio was reported within the ML treated specimens. It's important to point out that the Δh changes that are reported are for different cured specimens and not the deformation that occurs during the curing process. In both cases, the stress to volume change appears to be roughly linear.

Figure 5.6 presents a different look at the volume changes between the two bench tests by examining the changes in void ratios recorded between the cured specimens.

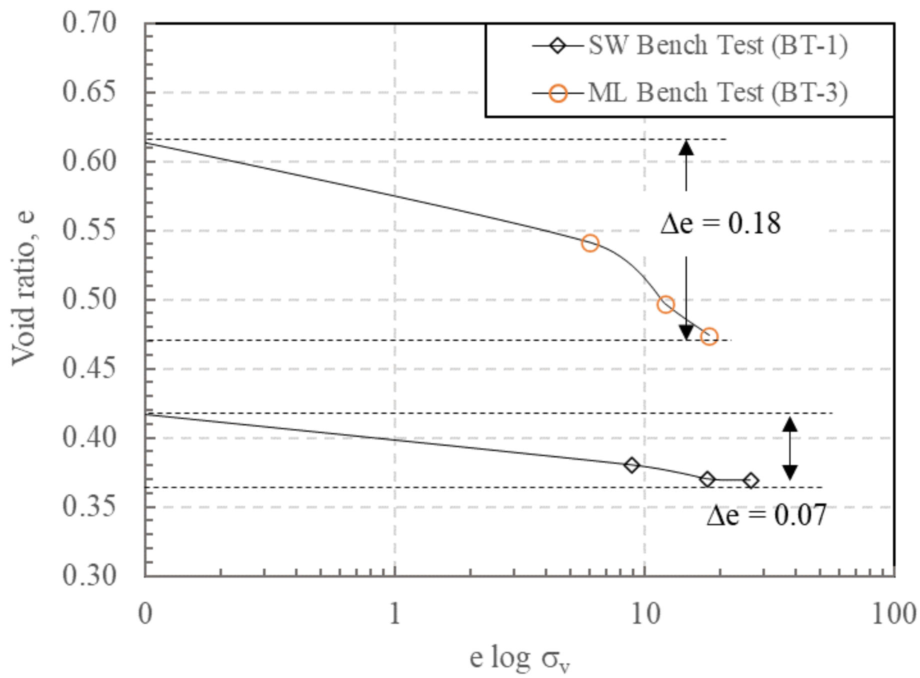

Figure 5.6 e log σ_v relationship between cured specimens for each treated soil type.

Based on the changes in void ratio between these two bench tests, consolidation of the SW specimens appears to be reaching a maximum, whereas the ML specimens were continuing to decrease. It can be theorized that hydraulic conductivity, k of the treated soil has significant a role in the amount of consolidation that can take place as the treated material cures, as the time at which consolidation can occur is limited by the cement hydration bonding taking place. Treated materials with greater permeability such as sands, can reach a denser state; however, this this does not necessarily correlate to higher strengths of the material, which is evident by the unconfined compressive strength results. Figure 5.7 shows the relationship between dry density of the specimens and curing stresses applied.

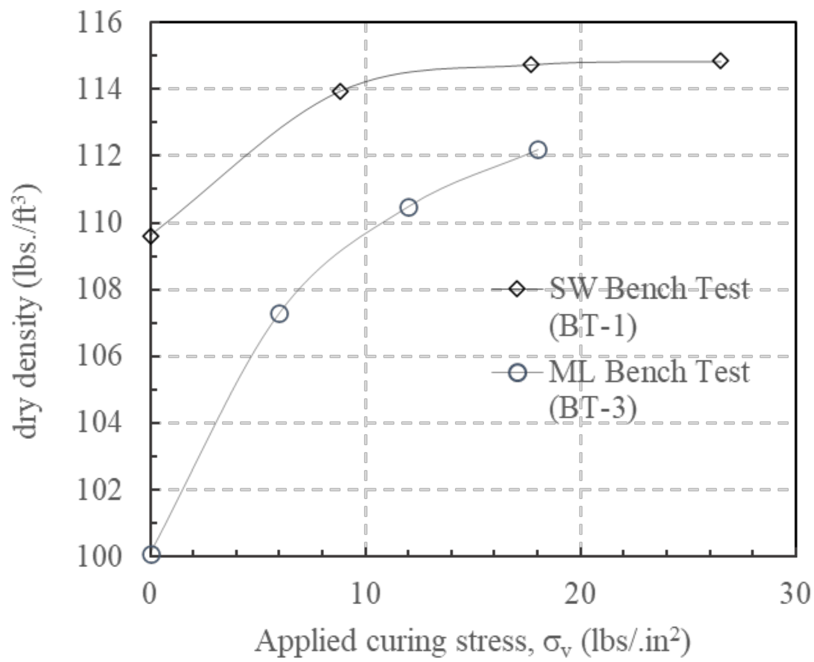

Figure 5.7 Relationship between dry density, γ_{dry} and applied curing stress, σ_v for SW and ML soils.

The information provided in Figure 5.7 shows that the granular soil reaches its point of maximum density at a much lower curing pressure compared to the fine-grained soil throughout the curing process. One possible explanation for this observation is the faster drainage of the specimens. On the other hand, for non-granular soils, such as cohesive soils (e.g., clayey soils), the drainage of water is slower due to smaller capillaries and attractive forces between the particles. Consequently, achieving the point of maximum density may require a higher curing pressure and a longer consolidation time. While this process seems to follow typical consolidation theory, it does not alone directly explain the mechanisms that are driving the greater rate of strength gains observed in fine-grained soils compared to granular soils.

5.3 Evaluation of Field Oedometer Data

It was found that approximately 80 percent of field oedometer exhibited a very strong correlation, with a linear squared regression (R^2) value of 0.75 or greater, indicating that the observed strength gains during testing were significantly influenced by the applied overburden curing stress. About 20 percent of the datasets showed R^2 values slightly below 0.75, and none of the validated datasets had an R^2 value of less than 0.5.

A total of 13 datasets met the Level 1 data validation rules established by the validation program. For comparison, the datasets were combined by specific soil types into a single linear regression model, this data is shown on Figure 5.8. Soil types include clayey sand (SC), clayey sand to lean clay (SC-ML), and lean clay/silt (CL-ML), and well graded sand and sandy-clay/silt (SW-SM). The best linear regression lines are shown on the figure for each of the combined soil type datasets. Linear regression fits for each of these datasets show *very strong* correlations that the rate of strength gains was influenced by curing pressures having R^2 values of 0.94 for the SC group, 0.92 for the SC-ML group, 0.91 for the CL-ML group, and 0.97 for the SW-SC group.

Figure 5.8 shows the relationships between the rate of strength gains to the applied curing stress for the four different soil group types. Slope equations for each of the datasets are also shown on the figure, showing slope coefficient that influences the rate of strength gain for each of these soil types. Each soil group represents slightly different gradation distributions from a blend of more granular soil (SW-SC) to primarily fine grain soil (ML-CL). For comparison, the data from the two bench tests are also shown on Figure 5.8 to compare bench test results against the broader field oedometer data. It's important to note that none of the soil groups contained highly plastic clay soils.

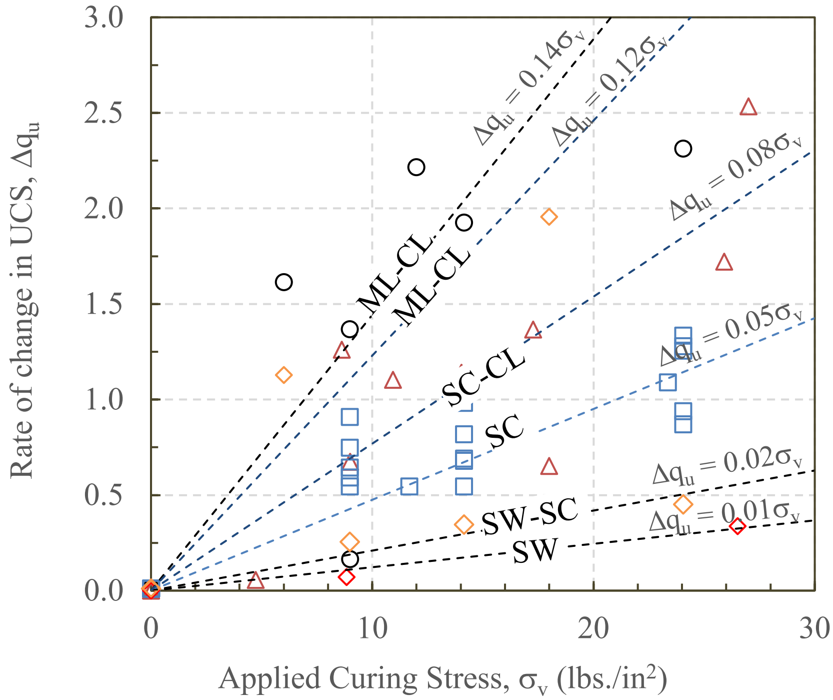

Figure 5.8 Comparison of the influence of soil type on the rate of strength gains, Δq_u from the field oedometer datasets

Based on a comparison of these results, the influence of soil type or more specifically grain size can be seen on the rate of strength gains. Cement treated soil with greater amounts of fine grain particles exhibit a higher rate of strength gained when cured under overburden stresses. As shown on Figure 5.8, the field oedometer results show a strong correlation with rate of strength gain relationship observed within the bench studies.

The relationships shown in Figure 5.8 allow for engineers to make reasonable empirical estimations of in-situ unconfined compressive strength based on a typical QC wet grab specimen cured at ambient atmospheric conditions, the treated soil type, and a depth of interest.

Equation 5.2 was derived to approximate a UCS value (q_u) at a certain depth based on a UCS value $q_{u,0}$, depth z, and the soil type being treated. To estimate a UCS value at depth, a dimensionless coefficient (α) can be used for the treated soil type. Table 5.3 provided a suggested α for soils that classify as SP, SW-SC, SC, SC-CL, and CL.

$$q_{u,predicted} = q_{u,0} + \frac{q_{u,0}(\sigma_z)}{\alpha} \quad (5.2)$$

Where, $q_{u,\ predicted}$ is the estimated UCS value at depth z, $q_{u,o}$ is the UCS value of a soil-cement specimen cured with no overburden pressure, α is the strength gain coefficient based on soil type (see table 5.3), and σ_v is the estimated overburden pressure at depth z (feet or meter). Curing pressure during the freshly mixed stage of deep mixed column is assumed to be hydrostatic, which can be estimated using Equation 5.3.

$$\sigma_z(z) = \gamma_{sc,\,wet}(z) \quad (5.3)$$

Where, $\gamma_{sc,wet}$ is the unit weight of freshly mixed (wet) soil-cement material, z is the depth of interest within the deep mixed column. Table 5.3 provides the range values of α, based on the soil type being treated. Predicted coefficient α represent a range of about +/- 20 percent in rate of strength gain within each soil type.

Table 5.3 Predicted Strength Gain Coefficient α

Soil Type	α
SP	>70
SW-SC	27 - 70
SC	16 - 27
SC-CL	11.5 - 16
CL	7 - 11.5
CL-ML	≤ 7

5.4 Comparison of Core Data to Predicted Δq_u

Coring data for this study is used as an independent verification. The objective is to confirm the findings of a study by collecting uncontrolled data from non-research specific sources. Independent verification is crucial to ensure the reliability and credibility of research outcomes, as it helps to determine if the observed effects are consistent with actual field conditions. The goal is to ensure that the findings are not simply the result of chance or bias and can be replicated or supported by other independent investigations. Independent verification provides an important means of assessing the robustness and accuracy of research findings and increasing confidence in the results.

As explained in Section 3.6, the imperative necessity of corroborating the coring data cannot be overstated, as it is paramount to ensure its portrayal of a nearly homogenous material. Failure to do so may lead to substantial distortion in the research outcomes.

The core datasets comprised of 21 core runs that satisfied the Level 0 data validation criteria described in Section 4. Among these datasets, approximately 62 percent of the unnormalized data exhibited a highly robust correlation (R^2 greater than 0.75) signifying a dependency of strength gain on overburden pressure during curing. Additionally, about 29 percent of the validated datasets demonstrated a good to strong correlation (R^2 between 0.5 and 0.75) as determined by the best linear square regression of the data. However, it is important to note that 10 percent of the data group exhibited an R^2 value lower than 0.5, indicating lower confidence in the correlation observed in these cases.

The presence of slightly lower R^2 values in the parametric regression analysis of the core data group was expected, considering the potential existence of confounding variables within the datasets, which might not have been identified during the Level 0 data validation review. These confounders could encompass unaccounted variations in additive binder rates between specimens, diverse soil conditions, or the influence of damage or inclusions in the tested coring specimens, all of which could impact the recorded strength values.

Despite these potential confounding factors, it is noteworthy that 90 percent of the overall data group still exhibited a significant and favorable correlation between confinement stress during curing and the strength values. Moreover, a substantial majority of the datasets included more than five individual depth variables, which considerably diminishes the likelihood of coincidental correlations. This strengthens the credibility of the observed relationships between confinement stress and strength values in the research findings.

To enhance the comprehension of the correlation, a non-parametric analysis using Spearman's rank correlation was conducted. This method is well-suited for assessing the strength of a relationship between two variables, particularly when dealing with monotonic functions, as observed in this study. The results of the analysis revealed a significant outcome, indicating that there is a high level of confidence (95.2 percent) in the existence of a very strong correlation between curing stress and the unconfined compressive strength values within the coring data group. This finding further reinforces and solidifies the relationship observed between these variables and bolsters the validity of the research conclusions.

Figure 5.9 presents this data graphically, while Table 5.4 provides a comparison of α coefficients calculated from the inverse of the slope of the linear regression lines for each soil type.

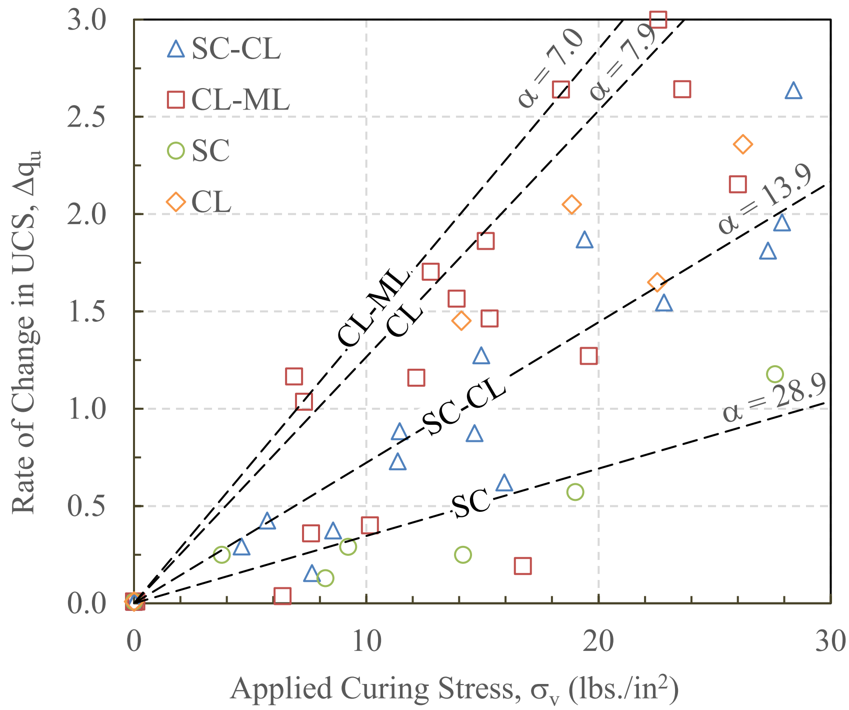

Figure 5.9 Estimated coefficient α values for soil types based on independent core run strength data.

These results show a strong correlation between the laboratory bench tests and the field oedometer strength gains for similar soil types. Table 5.4 presents a table that compares the estimated α values from the core data to the predicted range of α values.

Table 5.4 Comparison of coring data α to predicted α coefficients.

Soil Type	α (predicted)	α (Core data)
SW-SC	27 - 70	-
SC	16 - 27	28.9
SC-CL	11.5 - 16	13.9
CL	7 - 11.5	7.9
CL-ML	≥ 7	7.0

The coring group data showed excellent agreement to the predicted strength gains, with the slight exception of the SC dataset. In general, these results do confirm that in-situ strength gains in the field under uncontrolled conditions do exhibit the predicted strength gains in the field under the right conditions.

5.5 BT-3 Heat of Hydration Measurements

A preliminary assessment of the heat of hydration temperatures measured during the BT-3 bench test was compared against the measurements of the in-situ tests. The objective of this assessment was to determine if notable variations in curing conditions are present.

After analyzing the temperature ranges measured during the BT-3 study, it became evident that the data comprehensively captured the entire heat of hydration cycle for the reaction. Most of the heat generated during the hydration process seemed to be completed within about 24 hours. Subsequent temperature fluctuations seemed to be influenced by variations in atmospheric temperature within the laboratory environment. This influence was particularly notable in the consolidated cell specimens, which were more exposed to the daily temperature changes occurring within the laboratory. The unconsolidated specimen (cured under no stress), on the other hand, did not display these temperature fluctuations as the specimen was placed within a cooler, shielding it from direct exposure to changes in surface air temperatures.

By averaging the daily fluctuations between night and day, the ambient air temperature in the laboratory was estimated to be around 22.5 °C (72.5 °F) after about 36 hours. This temperature was considered as the concrete temperature at the start of the experiment (t_0 = 22.50 °C) and was used to compare the total heat generated during the cement reactions in-situ.

The temperature data records an initial rise in temperature changes then a steady drop until the concrete reaches' ambient laboratory room temperatures. The changes in temperatures can be directly attributed to the concrete hydration process that undergoes five recognized stages of cement hydration (*Mehta, P.K., and Monteiro, P.J.M., 2014).* The five stages of cement hydration include:

Stage I: Pre-induction period - This initial stage involves the period of initial heat release as the cement comes into contact with water, initiating the hydration process.

Stage II: Induction/Dormant period - During this stage, there is a temporary abatement or decrease in temperature, which can be observed after the initial heat release. It is also referred to as the dormant period.

Stage III: Acceleration period - This stage is characterized by a significant increase in temperature and is considered the strength-gaining phase of the hydration reaction. During this phase, the hydration process is in full swing, and the concrete gains strength rapidly.

Stage IV: Deceleration period - In this stage, the Calcium-Silicate-Hydrate (C-S-H) reaction has largely run its course, and temperatures start to decrease. This decrease in temperature is due to a reduction in ionic diffusion and is not a result of the C-S-H reaction itself.

Stage V: Steady-state period - This final stage marks the point where the rate of heat flow becomes relatively constant and complete. At this stage, the hydration process has reached a stable state.

The curing temperatures and stages of hydration are annotated in Figure 5.10 below shown for the first 24 hours of the experiment.

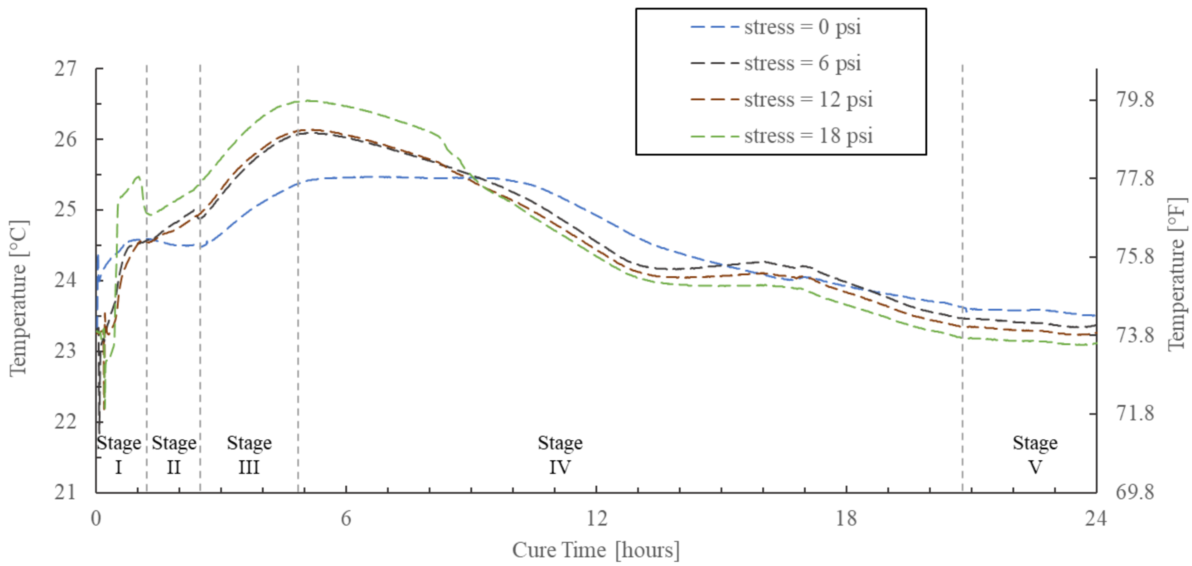

Figure 5.10 BT-3 Specimen curing temperatures and stages of hydration, first 24 hours.

Clear distinctions in hydration temperature are evident due to the varying levels of confinement pressure applied. Although these differences are subtle, Figure 5.10 demonstrates a discernible correlation between confinement stress and the heat of hydration. The specimens subjected to no confinement stress exhibited the lowest maximum temperature (25.41 °C), while the specimen under the greatest applied stress showed the highest maximum temperature (26.55 °C). Correspondingly, different confinement stresses led to distinct maximum temperature gains. This correlation is particularly noticeable during Stage 3, the acceleration period, which represents the strength gain phase of the hydration process.

In general, the temperature versus time sequence follows a somewhat typical pattern for concrete hydration, with maximum temperature ranges shown at about 5 hours after mixing. Further comparisons of these readings with in-situ temperature data collected from the field within an actual deep mixed column are provided in Section 5.7 below.

5.6 In-situ Stresses During Curing

As part of this study, the results of in-situ pressure cell measurements obtained from within two distinct deep mixed columns were analyzed. The primary objective was to gain valuable insights into the magnitudes and variations of internal lateral stresses occurring during the curing process. By analyzing these measurements, the author aimed to gain an understanding of the magnitude and changes in horizontal stresses that are occurring within the soil-concrete mass. The goal was to gain insight into the internal stresses that may be driving consolidation which is theorized may be responsible for the observed strength gains observed.

As detailed in Section 3, measurements of in-situ horizontal stresses commenced around the time when the deep mixed columns were freshly mixed. The timing of the data stream in relation to the curing phases of the material holds significant importance as it provides context due to the evolving phases of hydration occurring within the initial hours.

By initiating the stress measurements near the time of mixing, the study aimed to capture the dynamic changes in stress distribution and development during the early stages of curing. This period is critical as the cementitious material undergoes rapid hydration, transitioning from the plastic to the hardened state. Understanding the stress variations during this crucial time frame helps to characterize the consolidation processes within the deep mixed columns. These insights are essential for interpreting the mechanical behavior that could shed light on the strength gaining mechanisms that take place within the material during the early curing phases.

Figure 5.11 shows the changes internal horizontal stress (P_h data) for the first 22-hours post mixing for Site 1. P_h-data was converted into feet by dividing the wet unit weight of the soil-mixed material ($^{P}/_{\gamma_{sc,wet}}$). By converting into feet, the stresses can be viewed relative to ground surface. For site 1, the pressure cell was installed at a depth of 16.95 feet and groundwater was estimated to be about 3 feet below ground surface. By interpreting $P_h/\gamma_{sc,wet}$ (in feet), it can be observed that stresses at the pressure cell depth reached the total horizontal stress

(σ_h) based on the wet unit weight of the deep mixed material; thus, confirming an important assumption made in Equation 5.2.

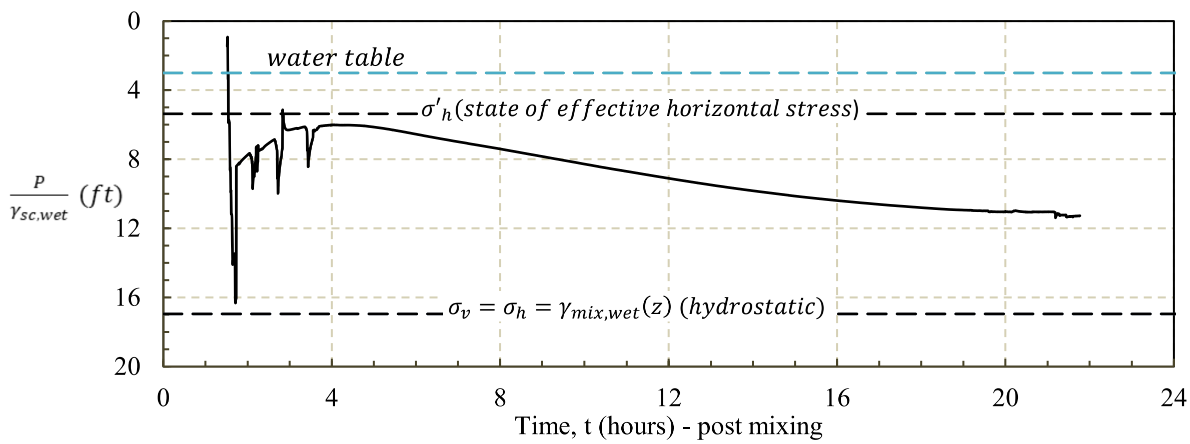

Figure 5.11 Site 1 Relationship between in-situ $P/\gamma_{sc,wet}$ data, total, and effective in-situ stresses versus time (t) post mixing – first 24 hours.

Considering Figure 5.11, it proves challenging to identify all the specific stresses that contribute to shaping the observed profile. Nonetheless, the measurements from both sites produced similar shapes. It can be reasonable assumed that when the probe is first inserted, the soil-cement column, in the fresh state, exhibits little to no shear strength, thus vertical and horizontal stresses are likely the same (hydrostatic). As the soil-cement mixture undergoes the hardening process, its shear strength progressively increases. Consequently, it can be inferred that horizontal stresses should likely be decreasing concurrently. The observed decrease in horizontal stress may be evidence of this process. It appears that horizonal stresses then reach a point of some state of effective horizontal stress before stresses start to increase again. The latter observation of increasing horizonal stresses is difficult to understand with additional information. However, it's conceivable to hypothesize that the soil-cement mixture might still be in a relatively plastic state, exhibiting behavior akin to that of an over-consolidated clay. In such a scenario, the coefficient of horizontal stress (K_o) could be on the rise, possibly reaching values of 1 or even greater. This hypothesis could potentially offer an explanation for the observed elevation in horizontal stress. Eventually once the soil-cement column completes its hardening process, it can be anticipated that the horizontal stresses within the mass will ultimately approach zero.

Figure 5.12 shows a similar horizontal stress pattern for Site 2. For this site, the pressure cell was installed to a depth of 16 feet, and the groundwater water was reported to be about 7.5 feet below ground surface. Total stresses were calculated based on an average unit weight of 105 lbs./ft^3 the wet deep mixed material.

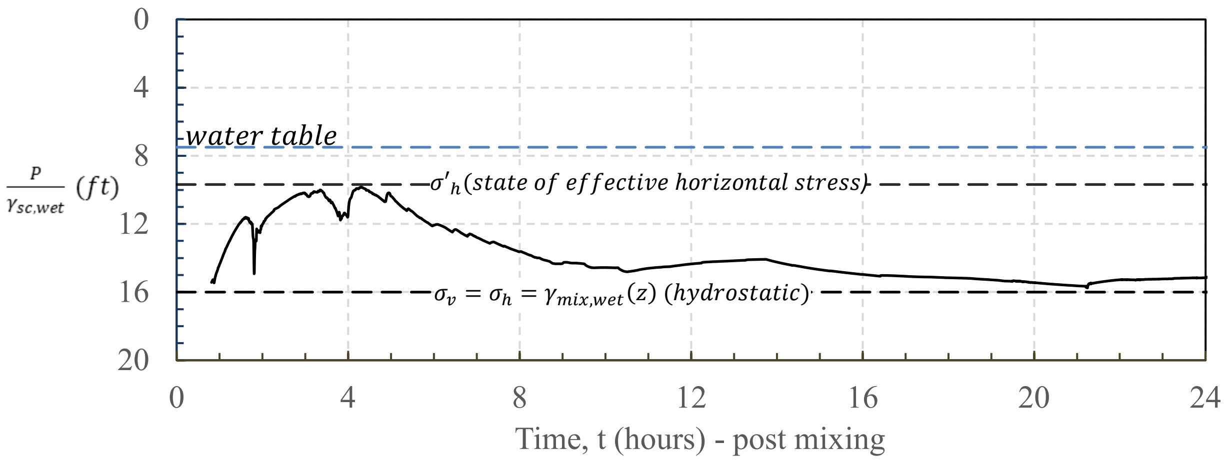

Figure 5.12 Site 2 Relationship between in-situ P/$\gamma_{sc,wet}$ data, total, and effective in-situ stresses versus time (t) post mixing – first 24 hours.

The pressure cell data from Site 2 reveals a notable similar pattern in changes in horizontal stresses. During this time, factors like consolidation and dissipation of excess pore pressures may also be factors affecting these stress changes.

The observed changes in internal horizontal stresses reflect a complex interplay of possibly drainage, consolidation, hydration reaction, drying, and soil structure reorganization.

5.7 Comparison of In-situ Heat of Hydration Temperatures to Bench Test Specimens' Temperatures.

Temperature measurements obtained from in-situ tests conducted at Sites 1 and 2 revealed surprising similarities, but they were notably different from the temperature profile recorded during Bench Test 3 (BT-3). It is essential to acknowledge that the treated soil types at Sites 1 and 2, as well as those used for BT-3, were coincidentally similar (classified as CL-ML). Furthermore, the binding rates and water-to-cement (w/c) ratios were also relatively similar. The similarities in binder content and w/c ratio are crucial factors to consider when evaluating the heat generated during the hydration processes, as they influence the activation energy (E_a) driving the heat released in the cement reaction. In general, higher binder rates would be expected to yield higher temperatures. The activation energy (E_a) is a parameter used to describe the temperature dependence of the rate of a chemical reaction. It is typically represented by the Arrhenius equation, shown as Equation 5.4:

$$k = Ae^{-E_a/RT} \tag{5.4}$$

Where k is the rate constant of the reaction, A is the pre-exponential factor (also known as the frequency factor), which represents the reaction rate at an absolute temperature of 0 K, E_a is the activation energy, which is the minimum energy required for the reaction to occur, e is the base of the natural logarithm (approximately 2.71828), R is the universal gas constant (8.314 J/(mol*K)), and T is the absolute temperature (in Kelvin) at which the reaction is taking place.

The Arrhenius equation is widely used in engineering to describe the temperature dependence of reaction rates. For the context of heat of hydration in soil-cement materials, the activation energy (E_a) plays a crucial role in quantifying how temperature affects the rate of strength development in the cementitious reaction.

Indeed, while a comprehensive isothermal calorimetric analysis falls beyond the scope of this study, the observation of temperature differences provides valuable insights into the variations in curing conditions. These differences shed light on how the curing environment may influence the strength development of materials. A comparison between materials cured within a controlled test cylinder setting and those cured in-situ helps identify the potential effects of different curing conditions on the final strength of the soil-cement mixture.

By examining the temperature discrepancies, a preliminary understanding of the heat of hydration contributes to the overall knowledge of how the cementitious reaction progresses in different curing settings and how the resultant strength may differ between laboratory-controlled conditions and actual field conditions. To compare the differences of generated heat of hydration at least broadly between these specimens, a look at only the change in temperature (ΔT) is needed. ΔT is defined by Equation 5.5.

$$\Delta T = T_t - T_0 \tag{5.5}$$

Where, ΔT is the change in Temperature (°C), T_t is the temperature of soil-cement at time t (°C), T_0 is the temperature of soil-cement at the start of the test (°C). Figure 5.13 presents the temperature differences (ΔT) for both the in-situ tests (Sites 1 and 2) and BT-3. The time scales for the in-situ tests have been adjusted on the figure to reflect the same curing phase post mixing.

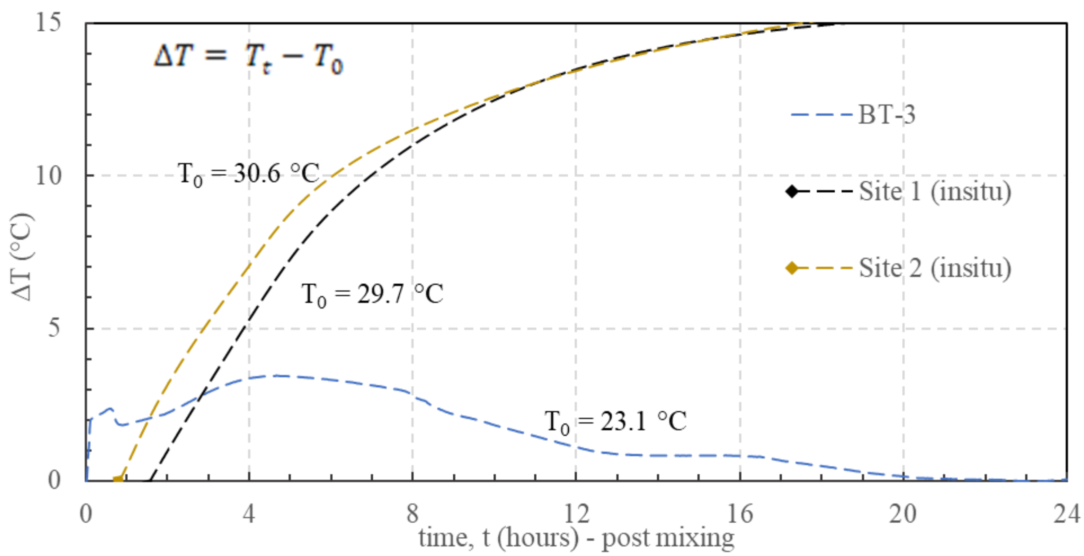

Figure 5.13 Comparison of ΔT between in-situ columns versus BT-3 specimen.

Based on a review of the temperature data, the heat generated during the bench study exhibited a typical chemical hydration pattern, while the heat recorded during both in-situ tests displayed significantly different patterns. At the most activated phase of hydration, observed at approximately $T_{4.5}$ hours, the in-situ temperature differences (ΔT) were 1.8 times higher for Site 1 and about 2.3 times higher for Site 2 compared to the standard concrete test cylinder.

The recorded temperature differences within the standard concrete test cylinder gradually decreased back to the initial temperature (T_0) as the deceleration and steady state phases were initiated. However, both in-situ temperature measurements showed a steady increase in temperatures beyond 24 hours, with temperatures continuing to rise for the entire duration of the tests. Åhnberg and Holm (1984) also reported in-situ temperatures with a lime and cement treated soil columns reaching temperature of about a hundred degree Celsius or more in the middle of the lime-treated soil column after installation and reported that temperatures in cement-treated columns continued for a longer period.

The effect of curing temperature on the strength of stabilized soil is not as straight forward as just a calorimetric quantification of activation energy, but rather varies with the type of soil that are treated (Åhnberg and Holm,1989). Åhnberg and Holm (1989) also suggested that the exact prediction of shear strength in-situ cannot be expected from unconfined compressive tests on samples stabilized in the laboratory because curing temperature would be significantly different. According to their study, a relatively good estimate of strength increase at varying curing temperatures can also be made by using the maturity number M_t. The equation for M_t is shown as Equation 5.6 (Åhnberg and Holm, 1984).

$$M_t = (20 + (T - 20)K\,)^2\sqrt{t} \tag{5.6}$$

Where, T is the curing temperature, °C, t is the time after stabilization, days, and K is a factor varying with the type of additive, soil, and temperature. Empirical values of K were suggested to be about 0.5 at temperatures higher than 20°C and 0-0.5 at temperatures from 8 °C up to 20°C. Åhnberg and Holm (1989) suggested that material strength can be estimated by plotting shear strength versus M_t to obtain strength with time after stabilization. While the method seems reasonable, it requires a lot of upfront testing and may not be accurate if site soil types vary in the field.

5.8 Comparative Analysis of the Effects of *w:c* Ratio on Δq_u

Authors of this study frequently receive comments regarding the field-induced stresses on specimens using the modified oedometer cells, particularly concerning whether the consolidation imposed by the apparatus may artificially reduce the effective water-to-cement (w/c) ratio and subsequently increase the strength of the specimens. In Section 5.7, it was inferred that consolidation of the deep mixed materials does occur during curing. However, the exact extent to which changes in the total water-to-cement (w_t:c) ratio alone contribute to the observed strength gains remains not fully understood.

The total water-to-cement ratio is defined as the sum of the weight of the water in the soil plus the weight of the water in the grout, divided by the weight of the cement in the grout. Although this research did not specifically address this topic with a dedicated laboratory program, this section introduces an analytical approach using empirical relationships developed by previous researchers to address this inquiry.

The central inquiry being addressed is whether the reduction in the water-to-cement ratio resulting from consolidation can account for the observed strength gains, or if there are other interparticle mechanisms at play that contribute to the increase in strength.

Drawing from a literature review, several studies conducted by Miura et al. (2001), Jacobson et al. (2003), Hodges et al. (2008), Filz et al. (2018), and Wei et al. (2018) have consistently demonstrated a positive correlation between unconfined compressive strength (UCS) and a decrease in the water-to-cement (w_T:c) ratio. Filz et al. (2018) have further proposed an empirical approximation for UCS using a power function based on the total water-to-cement ratio in the grout, as expressed in Equation 5.7.

$$\frac{UCS_{28\,day}}{p_a} = a_3(w_t{:}\,c)^{a_4} \tag{5.7}$$

Where, $UCS_{28\text{ days}}$ is the estimated unconfined compressive strength (UCS) at 28 days, w_t:c is the total water-to-cement ratio, p_a is atmospheric pressure, and a_3 and a_4 are dimensionless coefficients.

Through supplementary laboratory experiments conducted on specimens containing silt (ML-CL) as the base soil type, Filz et al. (2018) determined specific coefficients, namely a_3 and a_4, to be 2,000 and -1.55, respectively. These coefficients led to the derivation of Equation 5.8, which enables the estimation of unconfined compressive strength (UCS) at 28 days based on varying water-to-cement (wt:c) ratios.

$$UCS_{28\,day} = 2{,}000\,(w_t{:}c)^{-1.55} \tag{5.8}$$

In a related research study by Wei et al. (2018), a comparable exponential function for estimating UCS, as depicted in Equation 5.8, was presented. This function is applicable when considering a constant void ratio and binder content. It was clarified in the report that in Wei et al.'s work, the term "*w:c*" is equivalent to "w_t:*c*." To maintain consistency in the report, Equation 5.9 (*Wei et al., 2018*) was accordingly modified to represent the term as the "total water-to-cement content."

$$q_{uc} = A \cdot e^{-n_1} \cdot cc^{n_2} \cdot exp^{-n_3(w_t:c)} \tag{5.9}$$

Where, q_{uc} is the unconfined compressive strength, *CC* is the cement content (%), and *A*, n_1, n_2, and n_3 are all fitting parameters. Fitting parameters used for this evaluation are shown in Table 5.5.

Table 5.5 Fitting Parameters (*Wei et al., 2018*)

A	n_1	n_2	n_3	Void Ratio e	Cement Contant, CC (%)
130	2.84	1.06	0.66	0.557	20

In addition to the empirical correlations from Filz et al. (2018) and Wei et al. (2018), a third set of comparative data was incorporated into the study. This dataset comprises actual laboratory measured UCS values obtained from specimens mixed and tested with various water-to-cement (w:c) ratios. The data was obtained from an unrelated deep mix project mix design study and was donated for the purpose of this research. Coincidentally, the w:c ratios, cement content, and soil type used in this donated dataset align with the general range of the BT-3 study conducted with CL-ML soil. A binder factor of 115 kg/m^3 (7.18 lbs./ft^3) was used in the mix. Table 5.6 presents the measured 14-day UCS values for different *w:c* ratios used in the study.

Table 5.6 Relationship between *w:c* ratio versus measured $UCS_{14\ days}$

w:c	γ_{dry} (lbs./ft^3)	$UCS_{14\ days}$ (lbs./ft^2)
2.0	121.4	172.8
1.7	121.9	210.0
1.5	121.0	219.0

5.9 Estimation of Effective w_t:c Ratio from BT-3 Consolidation Data

The calculation of effective water-to-cement (w_t:c) ratios from the recorded consolidation data involves several key parameters and assumptions. These include:

Recorded Volumetric Changes: The volumetric changes of the specimens during consolidation are recorded and utilized in the calculations.

Mix Design *w:c* Ratio: The initial water-to-cement (w:c) ratio in the slurry used for mixing the specimens is considered.

Initial Water Content: The initial water content of the soil is taken into account in the calculations.

Specimen Saturation: The assumption is made that the wet mixed specimens are 100 percent saturated throughout the consolidation process.

Based on these parameters and assumptions, Table 5.7 presents the relevant data used to estimate the wt:c ratios for each specimen consolidated at different confinement stresses. The w_t:c calculations are based on a total mass of binder in each specimen, which was fixed at 173.2 grams.

Table 5.7 Calculated changes in effective w_t:c ratios due to specimen consolidation

Applied Curing Pressure σ_v (lbs./ft^2)	Height of Specimen h (in)	Volume of Specimen V (in^3)	Change in Volume ΔV (in^3)	Change in water weight ΔWw (g)	Total weight of water in specimen W_{wt} (g)	Calculated effective w_t:c
0	5.94	41.99	-	-	343.79	1.99
6	5.56	39.30	-2.69	-44.06	299.73	1.73
12	5.48	38.74	-3.25	-53.23	290.56	1.68
18	5.19	36.69	-5.30	-86.81	256.98	1.48

Table 5.8 shows the values of applied curing pressures, calculated effective wt:c ratios, and the measured UCS values from BT-3 study. It should be noted that the relationships between the three variables, namely overburden curing stress (σ_v), effective water-to-cement ratio (w_t:c), and unconfined compressive strength, are not fully understood and are somewhat complex. For example, σ_v and w_t:c: Changes in overburden curing stress (σ_v) can influence both the effective water-to-cement ratio and the unconfined compressive strength (UCS), but not necessarily by the same geo-mechanical mechanisms. As the overburden curing stress increases, consolidation affects movement of water within the specimen, this affecting the w_t:c ratio; however, changes in overburden curing stress (σ_v) cause densification and rearrangement of soil particles, leading to increased inter-particle bonding and, consequently, higher UCS values. Therefore, the relationship between the effective w_t:c and unconfined compressive strength is not as straightforward. While lower w_t:c ratios are often associated with higher UCS values due to reduced water content and improved cement hydration, this relationship is not universally linear. Other factors, such as the soil's specific surface area, curing conditions also influence UCS independently of the w_t:c ratio.

In summary, while overburden curing stress (σ_v) can affect both w_t:c and UCS, the relationship between w_t:c and UCS is more complex, and changes in the w_t:c ratio may not always result in proportional changes in UCS. Other factors and mechanisms are likely contributing to the observed changes in unconfined compressive strength.

Table 5.8 Summary of parameters and effective $w_t{:}c$ calculated for BT-3

Applied Curing Stress σ_v (lbs./ft^2)	Calculated effective $w_t{:}c$	Measured UCS (lbs./ft^2)
0	1.99	665
6	1.73	1,415
12	1.68	1,775
18	1.48	1,965

To evaluate these relationships, a plot of the effective water-to-cement ratios against the measured and empirical unconfined compressive strength values is made. The empirical equations 5.8 and 5.9 were used to estimate UCS based on the estimated w_t:c ratio calculated for the BT-3 consolidation data. The UCS values for the laboratory dataset, where specimens were mixed and tested with different water-to-cement ratios are also plotted against their corresponding effective w_t:c ratios. This enabled a fair comparison of UCS values cured without stress against the UCS values of the specimen cured with stress.

In the analysis, the UCS values were normalized using Equation 2.1 (Δq_u). This normalization was done to express the rate of strength gain for each dataset, utilizing the same effective water-to-cement ratios as calculated for the BT-3 study. The effective $w_t{:}c$ ratios used for normalization were 1.99, 1.73, 1.86, and 1.48, representing different points within the range of interest. This normalization allowed for a direct comparison of the strength gain rates among the datasets while considering the variations in the effective $w_t{:}c$ ratios. Figure 5.14 shows the relationship between $w_t{:}c$ ratio and the empirical and measured rate of strength increase (Δq_u) between both unconsolidated specimens and consolidated specimens.

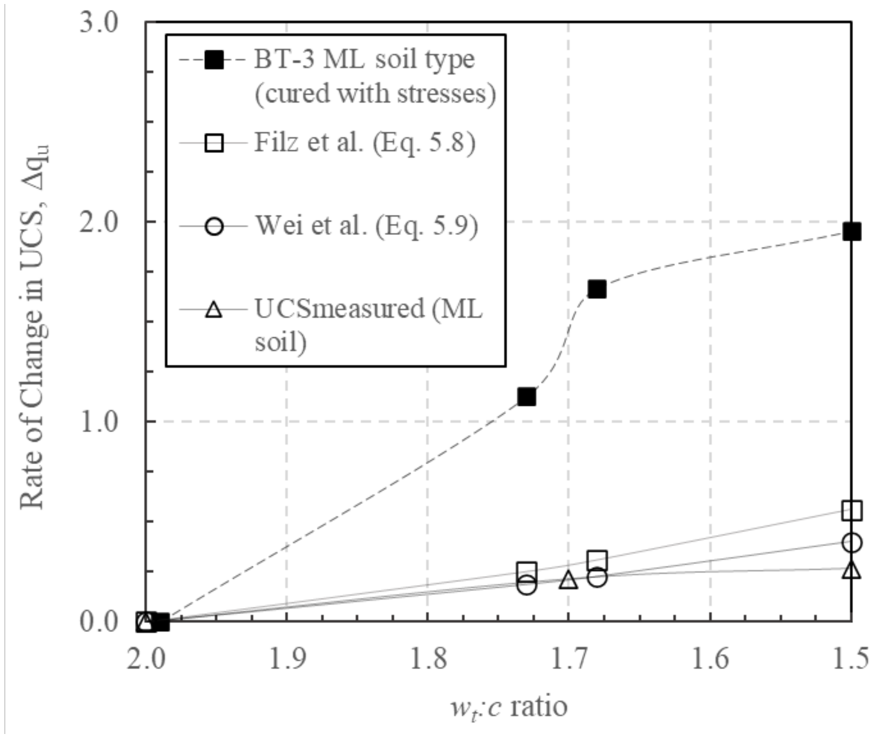

Figure 5.14 Relationship between changes in w_t:c ratio and Δq_u for specimens cured with and without overburden stress for ML type soil.

The results of the analysis reveal a significant difference in the rate of strength gain observed for the BT-3 dataset, which was cured under overburden curing stress, compared to the strength gains obtained from the comparative datasets representing specimens cured without curing stresses. Specifically, the empirical equations (5.8 and 5.9) and the measured UCS dataset all exhibited consistent agreement with each other concerning the effect of the w_t:c ratio on the rate of strength gains.

In Section 5.2, it was shown that the Δq_u value for BT-3 falls within the typical range of strength gains predicted for low plasticity fine grain soils, as observed throughout the study. However, it is important to emphasize that the strength gains observed in the BT-3 dataset, representative of low plasticity fine grain soils cured under confining stress, cannot solely be attributed to changes in the w_t:c ratio. Other contributing factors beyond the changes in the w_t:c ratio must be considered to explain the observed strength gains.

CHAPTER 6

CONCLUSIONS

Based on a review of the results, observations, and analyses conducted in presented in Chapter 5, the following key conclusions and answers to the research questions are discussed:

6.1 Influence of Internal Curing Stresses on the Strength of Cement-treated Soil

1. *What are the internal stresses within a deep mixed column and how do they change from the point that soils are first treated throughout the curing process and does this process influence material strength?*

Internal stresses within a deep mixed column appear to involve a complex interplay of hydration reactions, drying, and soil structure reorganization as the soil-cement materials consolidates, resulting in changes to the soil's mechanical properties. In-situ horizontal stress data appear to reveal a period when vertical and horizontal stresses may be hydrostatic in its initial fresh state, however, as the stabilizing agents harden, changes in horizontal stresses are decreasing until reaching a state of minimum effective horizontal stress. The actual contribution to this minimum effective stress is difficult to discern based only on the P_h -data.

2. *What influence does curing stress have on the strength of deep mixed materials?*

Curing stress in deep mixed materials promotes essential chemical and physical processes, including hydration, particle bonding, and consolidation. These processes work together to develop stronger interparticle bonds, leading to an increase in the material's overall strength as the material cures. As the curing process progresses, the cementitious binder grows (formation of calcium silicate hydrate crystals) and binds the soil particles together, creating interparticle bonds. This interlocking of particles enhances the cohesion and internal friction within the mixture, resulting in increased strength.

3. *Under curing stress, does grain size and plasticity of the treated soil affect the strength of the deep mixed material?*

Grain size, or more specifically, particle surface area, appears to play a significant role in influencing stronger cement bonding in a deep mixed soil-cement column. The surface area of the soil particles directly affects the amount of contact available for interaction with the cementitious binder. A higher particle surface area results in more available sites for cement particles to adhere to and form chemical bonds. This phenomenon is enhanced by the application of curing stresses which drives consolidation of the soil particles; thus, increasing the contact points. This increased contact enhances the opportunities for cement particles to attach to the soil particles, promoting better bonding. In addition, the increased surface area of smaller soil particles allows for more efficient water-cement interaction during the hydration process. This means that a higher proportion of cement particles can undergo hydration, leading to the formation of more cementitious compounds that contribute to bonding. In fact, the empirically derived coefficient α appears to provide a reasonably quantification of the contribution of grain sizes on strength. It should be noted that the limitations of applying the strength gain coefficient, α is limited to about 30 psi.

These conclusions are reinforced by the parametric analysis examining the influence of $w_t{:}c$ on the rate of strength gain. The analysis demonstrated that the rate of strength increase observed in the treatment of low plasticity clays far exceeded what would be expected solely from changes in the wt:c ratio. These findings strongly suggest that confinement stress during curing triggers other interparticle mechanism(s) that play a significant role in driving the observed strength gains.

The parametric analysis provides compelling evidence that factors beyond changes in the $w_t{:}c$ ratio are at work in strengthening soils with different grain size distributions. The presence of confinement stress during curing appears to activate additional mechanisms that contribute substantially to the observed increase in strength based on the soil type. These findings shed light on the complexities of deep mixing and emphasize the importance of considering multiple factors in understanding the strength development of treated soils.

This study also reveals that fine-grain soils with high plasticity exhibit a limiting or counteracting effect on the role that curing stresses have in promoting interparticle bonding. The high plasticity clays hinder rapid drainage, leading to a lack of consolidation and, consequently, preventing closer bonding of the soil particles. As a result, the expected strength gains are not achieved.

Moreover, mixing high plasticity clays presents challenges, leading to a non-uniform and heterogeneous composition of the material. This non-uniformity results in more erratic and highly variable strength outcomes, further complicating the prediction of material performance.

In summary, the presence of high plasticity clays in fine-grain soils hinders the beneficial effects of curing stresses on interparticle bonding, leading to limited strength gains. The difficulties in mixing such clays add to the variability of strength results, making the behavior of these soils more unpredictable and challenging for ground improvement applications.

6.2 Influence of Hydration Temperatures on the Strength of Cement-treated Soil

4. *What are the hydration temperatures within a deep mixed columns and do they differ from specimens cured within a typical QC test cylinder?*

A direct comparison between the liberation of heat during hydration for soil-cement materials cured in situ and those cured within a typical concrete test mold. The results showed a striking difference in heat profiles between these two conditions. In-situ soil mixed columns exhibited significantly higher temperatures that extended far beyond 24 hours post-mixing, while specimens cured in the laboratory reached their maximum temperature at around 5 hours post-mixing.

The elevated temperatures observed in the in-situ conditions are attributed to the retention of heat from the hydration process of adjacent deep mixed columns and the thermal insulation provided by the surrounding ground. However, the implications of these higher ground temperatures on the overall strength development remain unclear. It is uncertain whether the typical in-situ curing process significantly influences greater strengths overall.

Based on a review of published literature, higher temperatures during hydration could potentially induce an acceleration effect on the early strength development of the material (Carino et al., 2001). Nevertheless, further research is required to confirm and better understand the impact of elevated temperatures in the ground on the strength development of soil-cement materials.

CHAPTER 7
RECOMMENDATIONS FOR FUTURE RESEARCH

This chapter presents recommendations for future research based on the conclusions made in this report: (1) effects of hydration and environmental temperatures on UCS long-term and short-term strength; and (2) future research to quantify the contribution of soil's specific surface area to the observed strength gains.

7.1 Effects of Hydration and Environmental Temperatures on UCS Long-term and Short-term Strength

This research superficially uncovers the disparity between in-situ and laboratory curing temperatures in deep mixed materials. The study compares the curing conditions experienced on construction sites (in-situ) with the controlled conditions in a laboratory setting where typical concrete test cylinders are cured. The study highlights the significant disparity in curing temperatures and explores their effects on the material's strength. Due to the limited understanding of the influence that temperature has on short-term and long-term Unconfined Compressive Strength values, the author recommends further field and laboratory studies with a focus on the effects of environmental curing temperatures on material strength. The study should include both short-term UCS values and the correlation with curing temperatures and long-term strength development and temperature influence, along with a study of the microstructure changes and their implications on material strength under both short- and long-term conditions. Once better understood, the research suggests the potential application of UCS correction factors for wet grab quality control samples.

7.2 Quantify the Contribution of Soil's Specific Surface Area to the Observed Strength Gains.

The research uncovered a compelling phenomenon, which involves the relationship between curing stress and soil specific surface area (SSA) in deep mixed materials. This relationship significantly influences the rate of strength gains within a deep mixed column. The phenomenon arises from a complex interplay of cement chemical bonding and interparticle deformation behavior, making it challenging to fully understand.

The hypothesis proposes that during the consolidation of cement-treated soils in their fresh state, silt and clay particles may align perpendicular to the normal load, leading to an increase in surface area (or contact points). This increased surface area promotes stronger cement bonding, driving the observed rate of strength gains in the material.

To quantify the effects of specific surface area on strength during consolidation of cement-treated soils, a multifaceted investigation, including several testing methods, can be employed. The recommended testing program would include X-ray Diffraction (XRD) analysis to identify the mineralogical composition of the cement-treated soil samples. This analysis will help understand the orientation and arrangement of clay minerals cured at different stresses and quantify their potential influence on cement bonding. Additionally, Scanning Electron Microscopy (SEM) can be used for observing the microstructures within the cement-treated soil samples, providing insight into particle alignment, surface textures, and the distribution of cementitious materials.

For further validation, it is suggested that the research program includes Mercury Intrusion Porosimetry (MIP) or similar methods to measure the pore size distribution and specific surface area of the cement-treated soil samples. This data can support the theory of increased surface area and stronger cement bonding. Moreover, combining MIP analysis with additional Unconfined Compressive Strength (UCS) testing using the modified oedometer apparatus at various curing stress levels will help quantify the relationship between curing stress, specific surface area, and the rate of strength gains.

The integration of these testing methods can effectively validate the theory and establish a better understanding of the complex interplay between cement chemical bonding, interparticle deformation behavior, curing stress, and specific surface area in deep mixed materials. Such insights will contribute significantly to the understanding of the behavior of cement-treated soils and provide better predictability of their engineering properties.

7.3 Coauthor Contributions

Giovanni Bonita, Ph.D., P.E., P.G. of GEI Consultants provided technical reviews for the referenced DFI Research Reports mentioned in several sections of this report.

REFERENCES

1. Åhnberg, H., Bengtsson, P., and Holm, G. (1989). "*Prediction of strength of lime columns*" 12th International Conference on Soil Mechanics and Foundation Engineering (Rio De Janeiro)

2. Bruce, M. E. C., Berg, R., Collin, J., Filz, G., Terashi, M., Yang, D. (2013) FHWA-HRT-13-046, *Federal Highway Administration Design Manual: Deep Mixing for Embankment and Foundation Support.*

3. Carino, N.J., Lew., H.S., (2001), The Maturity Method: From Theory to Application, Proceedings of the 2001 Structures Congress and Exposition, May 21-23, 2001, Washington, D.C., American Society of Civil Engineers, Reason, Virginia, Peter C. Chang, Editor, 2001, 19 P.

4. Daas P., Tennekes M., Zhang L.C. , Hendriks C., Foldal Haugen K., Cerroni F., Di Bella G, Laitila T., Wallgren A. and Wallgren B. (2011) Report on methods preferred for the quality indicators of administrative data sources. Deliverable 4.2 of the BLUE-ETS project.

5. Fang, K. Fall, M. (2019), Sh*ear Behavior of the Interface Between Rock and Cement Backfill: Effect of Curing Stress, Drainage Condition and Backfill Rate*, Rock Mechanics and Rock Engineering (2020), 53:325-336, https://doi.org/10.1007/s00603-019-01909-2

6. Hayashi, Y., Suzuki, A., Kitazono, Y. (2005), *Consolidation characteristics of the cement-treated soil in fresh state*, proceedings of the International Conference on Deep Mixing – Best Practices and Recent Advances, Deep Mixing '05, Stockholm, Sweden, May 25 – 25, 2005

7. Hirabayashi, H., Taguchi, H., Tokunaga, S., Shinkawa, N., Fujita, T., Inagawa, H., and Yasuoka, N. (2009). "Laboratory Mixing Test on Slurry Preparation, Specimen Preparation and Curing Temperature." Proc. of the International Symposium on Deep Mixing & Admixture Stabilization, Okinawa.

8. Mehta, P.K., and Monteiro, P.J.M. (2014). Concrete: Microstructure, Properties, and Materials (Fourth Edition). McGraw-Hill Education

9. Nevárez-Garibaldi. R, Miller, D., and Filz, G. (2018), *Influences of Mixture Proportions and Test Conditions on the Strength and Stiffness of Wet-Mixed Soil and Cement*, Report to the Deep Foundations Institute.

10. Onorato, G, Bonita, G. (2020), *Effect of Curing Stresses on the Mechanical Properties of Soil-Cement Mixed Materials*, DFI Research Summary Report, Deep Foundations Institute.

11. Onorato, G, Bonita, G. (2023), *Final Report on Continued Research on the Effect of Curing Stresses on the Mechanical Properties of Soil-Cement Mixed Materials*, DFI Research Summary Report, Deep Foundations Institute.

12. Rabbii, A. T. Z., Kuwano, J., Deng, J., and Boon, T. W. (2011), *Effect of Curing Stress and Period on the Mechanical Properties Cement-Mixed Sand*, Japanese Geotechnical Society, Soil and Foundations, Vol. 51, No. 4, pp. 651-661.

13. Suzuiki M, Fujimoto T., Taguchi T., (2014) *Peak and Residual Strength Characteristics of Cement-Treated Soil Cured Under Different Consolidation Conditions.* The Japanese Geotechnical Society, Soils and Foundation Publications, issue 54(4): pages 687-698, by Elsevier Publications,

14. Starcher, R. D. (2013). *Impact of Curing Time and Curing Stress on the Mechanical Behavior of Cement-Improved and Cement-Fiber-Improved Soft Soil* (Master's thesis)

15. Wei, X, Ku, T. (2019), *New design chart for geotechnical ground improvement: characterizing cement-stabilized sand*, Springer-Verlag GmbH Germany, part of Springer Nature 2019, published June 19, 2019.

APPENDIX A

PERMISSIONS FOR MATERIAL USE

A.1 Coauthor Permission

Coauthor permission to include Figures, Table, and data reproduced from other published sources is included below.

1) Coauthor permission to use figure, tables, and data used in previous publications.

8/8/23, 1:39 PM Mail - Onorato, George - Outlook

RE: Request Coauthor Permission for My Thesis

Bonita, Giovanni <gbonita@geiconsultants.com>
Tue 8/8/2023 1:16 PM
To:Onorato, George <gonorato@geiconsultants.com>

Sure George

GEI | GIOVANNI BONITA, PHD, PE, PG, PENG
Senior Vice President
202.828.9511 | cell: 301.717.3999
1615 L Street, NW, Suite 630, Washington, DC 20036-5750

From: Onorato, George <gonorato@geiconsultants.com>
Sent: Monday, August 7, 2023 7:30 PM
To: Bonita, Giovanni <gbonita@geiconsultants.com>
Subject: Request Coauthor Permission for My Thesis

Hello Giovanni -

I am writing to request your permission as a co-author for both the preliminary summary and final research reports on the "Effects of Curing Stresses on the Mechanical Properties of Soil-Cement Materials," with the second report pending publication. I would like to cite the tables, figures, and data used within those reports for my thesis.

It's my understanding that a reply to this email with your permission should be sufficient.

Thanks, let me know if you have any questions.

George

GEI | GEORGE A. ONORATO, P.E.
Senior Engineer
303.264.1064 | cell: 813.404.6688
4601 DTC Boulevard, Suite 325, Denver, CO 80237

A.2 Copyright and Contributor Permissions

Permission to include previously published material in this thesis is below.

1) Permission to use Figure 2.1 by Kitazume, M (2022).

8/8/23, 8:02 AM marketplace.copyright.com/rs-ui-web/mp/license/e5b63efc-846d-4336-9311-d6975e37e079/b501b87f-da32-4aa9-8aba-67e99075cbf5

CCC Marketplace

This is a License Agreement between George Onorato/Colorado School of Mines ("User") and Copyright Clearance Center, Inc. ("CCC") on behalf of the Rightsholder identified in the order details below. The license consists of the order details, the Marketplace Permissions General Terms and Conditions below, and any Rightsholder Terms and Conditions which are included below.

All payments must be made in full to CCC in accordance with the Marketplace Permissions General Terms and Conditions below.

Order Date	08-Aug-2023	Type of Use	Republish in a thesis/dissertation
Order License ID	1384074-1	Publisher	Taylor and Francis (Books) Limited UK
ISBN-13	9781032121048	Portion	Chart/graph/table/figure

LICENSED CONTENT

Publication Title	Quality Control and Assurance of the Deep Mixing Method	Language	English
Author/Editor	Kitazume, Masaki	Rightsholder	Taylor & Francis Informa UK Ltd - Books
Date	02/14/2022	Publication Type	Book

REQUEST DETAILS

Portion Type	Chart/graph/table/figure	Distribution	Worldwide
Number of Charts / Graphs / Tables / Figures Requested	1	Translation	Original language of publication
Format (select all that apply)	Electronic	Copies for the Disabled?	No
Who Will Republish the Content?	Academic institution	Minor Editing Privileges?	No
Duration of Use	Life of current edition	Incidental Promotional Use?	No
Lifetime Unit Quantity	Up to 499	Currency	USD
Rights Requested	Main product		

NEW WORK DETAILS

Title	QUANTIFYING THE EFFECTS OF CURING STRESSES AND SOIL TYPE ON THE IN-SITU COMPRESSIVE STRENGTH OF CEMENT-TREATED SOILS VIA DEEP MIXING METHOD	Institution Name	Colorado School of Mines
Instructor Name	Ning Lu, Ph.D.	Expected Presentation Date	2023-08-17

2) Permission to use coring data provided by Treviicos.

8/8/23, 2:18 PM Mail - Onorato, George - Outlook

RE: [EXT] Permission to use core data for my academic thesis

Wesley Schmutzler <WSchmutzler@treviicos.com>
Tue 8/8/2023 2:17 PM
To:Onorato, George <gonorato@geiconsultants.com>
Cc:Matthew Glisson <mglisson@dfi.org>

EXTERNAL EMAIL

George

There is no issue with the use of this data for incorporation into your thesis.
Good Luck!

Thanks

Wesley Schmutzler | Project Executive
TREVIICOS | 38 Third Avenue, 3rd Floor | Charlestown, MA 02129
(617)-241-4800 (office) (617) -620-4392 (cell)

3) Permission to use coring and field data provided by Bauer foundations.

8/13/23, 5:38 PM Mail - Onorato, George - Outlook

[EXT] RE: Permission to use data for my academic thesis

Arnold, Michael <marnold@bauerfoundations.com>
Sun 8/13/2023 11:50 AM
To:Onorato, George <gonorato@geiconsultants.com>
Cc:Matthew Glisson <mglisson@dfi.org>

EXTERNAL EMAIL

Hi George,

Thank you, I'm doing well.

Please take this as permission to utilize the HHD TO5 soil mixing data provided within the DFI Research Report on the effects of curing stresses on soil mixed properties for your graduate thesis. It would be great if you could share your thesis once completed.

Best regards and best of luck with your thesis!
Michael

Dr. Michael Arnold
Chief Engineer

Direct: +1 (813) 792-3368
Cell: +1 (561) 596-5957

michael.arnold@bauerfoundations.com
www.bauerfoundations.com

4) Permission to use coring and field data provided by Kiewit.

8/9/23, 8:46 AM [EXT] RE: Permission to using data for academic thesis - Onorato, George - Outlook

[EXT] RE: Permission to using data for academic thesis

Keith.Mattecheck <Keith.Mattecheck@kiewit.com>
Wed 8/9/2023 8:45 AM
To:Onorato, George <gonorato@geiconsultants.com>
Cc:Matthew Glisson <mglisson@dfi.org>

EXTERNAL EMAIL

Thanks for reconfirming our commitment to you using the data from our project. I understand that the data has been scrubbed so the project sites are not able to be determined. As discussed, you can use the data under the conditions outlined. Good luck with wrapping up your research.

Keith Mattecheck
SOE Lead, BSVII CP2 Tunnel/Trackwork

KIEWIT SHEA TRAYLOR, A JOINT VENTURE
2830 De La Cruz, Santa Clara, CA 95050
402-709-3106 cell
keith.mattecheck@kstjv.com

5) Permission to use published figures, tables, and data from the Deep Foundations Institute.

[EXT] RE: Publishing permission

Matthew Glisson <mglisson@dfi.org>
Fri 8/11/2023 9:30 AM
To:Onorato, George <gonorato@geiconsultants.com>;ADMCONSULT <ADMCONSULT@MSN.COM>

EXTERNAL EMAIL

Absolutely no worries, George! I know folks have to take care of the stuff that brings money in the door before the volunteer efforts.

Thanks for the information on publications for the 2018 project. For now, we will craft the permission assuming we publish a committee research report, a conference paper and a Deep Foundations magazine article, but no DFI Journal article.

Have a great weekend!
Matt

Matthew R. Glisson, P.E. | **O**: (973) 423-4030 | **Deep Foundations Institute**
Director of Technical Activities | **D**: (314) 707-3767 | 326 Lafayette Avenue | Hawthorne, NJ 07506